ALGERIAN DEMOCRATIC AND POPULAR REPUBLIC
MINISTRY OF HIGHER EDUCATION AND SCIENTIFIC RESEARCH
UNIVERSITY OF MOHAMED BOUDIAF – M'SILA

FACULTY OF SCIENCES
DEPARTMENT OF PHYSICS
N°: Ph/MAT/21/2020

DOMAINE: SCIENCE OF MATTER
FIELD: PHYSICS
OPTION: MATERIAL PHYSICS

Memory Submitted for Obtaining

Diploma of Academic Master

Prepared by: DEBAB ADALA

TITLE:

Study of the phase transitions and crystallization Kinetic Parameters of mixtures Al_2O_3-MgO-SiO_2

Defended on: 07/10/2020 before the jury composed of:

HERAIZ Menad	University of Msila	president of the jury
OUALI Ameur	University of Msila	Supervisor
SAHNOUNE Foudil	University of Msila	Examiner
ALLALI Djamel	University of Msila	Examiner

Academic Year: 2019/2020

Dedication

This work is dedicated to my family for the support they have provided me at all levels of my academic life, and I thank my classmates for their encouragement and support, I will continue walking even if the road I am walking is lonely, no one is perfect in the world, so I will smile myself proudly.

Acknowledgments

First of all, I thank God for his grace and help

I extend my sincere thanks with all the appreciation and respect that this word bears for everyone who helped me in this work in particular Professors / **HERAIZ Menad** and **OUALI Ameur** for their constant supervision and follow-up to us throughout the completion of this research, their continuous support, patience and motivation. I also extend my sincere thanks to each of the respected Professor **SAHNOUNE Foudil** for his unlimited work, help, valuable advice, directions, and encouragement to him.

I wish also to express my gratitude and thanks to **Sahnoune Foudil, Hraiz Menad, OUALI Ameur** and **ALLALI Djamel** for their acceptance to judge this work.

I thank the professors for everything they have done for me

I would also like to thank the members of the discussion committee

I also thank all the professors from whom I have learned at least one **letter**

I would like to thank all the professors and colleagues at the Physics Lab at the University of M'sila for all their support, encouragement and advice.

Thanks to my friends and colleagues at M'sila University.

Index

Index

CHAPTER II: Experimental methods used and devices used

Index

Chapter III: Experimental results and discussion

General Introduction

Introduction

Ceramics is a solid inorganic and non-metallic, consisting of metallic or non-metallic compounds that are formed and then hardened by heating to high temperatures. In general, they are hard, wear-resistant and brittle materials. These advanced and technical ceramics are used in applications such as space shuttle tiles, engine components, artificial bones and teeth, computer hardware components, cutting tools, etc. The special character of ceramic materials leads to many applications in materials engineering, electrical, chemistry, engineering and mechanical engineering. Because ceramic is heat resistant, it can be used for many jobs that materials such as metals and polymers do not fit. Ceramic materials are used in a variety of industries. Among the most popular technical ceramics are cordierite and mullite ceramics .

Cordierite ($2MgO\ 2Al_2O_3\ 5SiO_2$) is an important naturally occurring ceramic material, which is especially popular for its extraordinarily low thermal expansion coefficient, low thermal mass, low thermal conductivity coefficient (high thermal insulation constant), and great chemical stability which means high resistance to corrosion, High tensile strength, high toughness, high fracture resistance, high dielectric stability, and excellent thermal shock resistance.

Mullite is the mineral name for the only chemically stable intermediate phase in the SiO_2 - Al_2O_3 system. The mineral rarely occurs in its natural form, and mullite is usually represented as $3Al_2O_3{\cdot}2SiO_2$, various starting materials and preparation techniques are used to produce synthetic mullite ceramics. The properties of mullite are subject to the raw materials used and the technology for their preparation. In general, the largest application of mullite-based products is in refractories. In the steel and glass industries, it is the most widely used refractory material. Due to its excellent physical and chemical properties, it possesses high thermal insulation, poor electrical conductivity, weak linear expansion coefficient, as well as good chemical stability and thermal shock resistance.

In our research, we prepared laboratory samples of mixtures of cordierite-mullite compounds. This humble research is divided into three chapters:

General Introduction

The first chapter is a reference study in which the definitions, properties, uses, and methods of preparing cordierite, mullite and cordierite-mullite are covered.

In the second chapter, we presented the experimental methods used in the process of preparing the cordierite - mullite compound with Soul-Gel technology, as well as in the manufacture and study of samples by following a set of methods and treating them with different devices.

As for the third chapter, it was devoted to presenting and discussing the results obtained, as we dealt with the following:

- Study the results of differential thermal analysis and the mass of the compound.
- Study the results obtained using a dilatometric of the prepared compound and know the phases formed and the expansion and contraction of the material at different temperatures and speeds.
- Calculation of the activation energy of α-cordierite and spinel.

In addition to the above, the paper contains an introduction in which we dealt with the importance of the topic, the presentation of the problem, the structure of the memo, and the proposed methods for solving the problem. We also ended the note with a conclusion that was a summary of our most important findings in Chapter Three.

Chapter I: Bibliographic study

In this chapter we will look at the generalities about ceramics, some definitions and properties of mullite and cordierite, as well as the mullite-cordierite compound, as well as methods for their preparation, and in the end we will discuss how to calculate the activation energy.

I. 1 Introduction

Ceramics can be defined as solid compounds that are formed by the application of heat, and sometimes heat and pressure, comprising at least two elements provided one of them is a non-metal or a nonmetallic elemental solid. The other element(s) may be a metal(s) or another nonmetallic elemental solid(s), a somewhat simpler definition was given by Kingery who defined ceramics as, "the art and science of making and using solids that contain a basic component and consist in large part of inorganic non-metallic materials" [1]. Haas also defined ceramics as materials produced by pouring powder and solidifying the shape through exposure to high temperatures, ceramics are distinguished by high resistance to corrosion and thermomechanical strength [1]. Ceramic materials can also be classified into two types according to the type of raw material and sorted according to composition: clay, oxide ceramics, non-oxidized ceramics, silicate ceramics (steatite, cordierite) [2].

I. 2 Cordierite

I. 2. 1 Definition of cordierite

Since its discovery in 1813, cordierite ($2MgO_2.Al_2O_3.5SiO_2$), named after the French geologist Pierre-Louis-Antoine Cordier (1777-1861), has been the subject of extensive research. What makes cordierite most unique is its very low thermal expansion coefficient, and excellent resistance to thermal shock [3]. Cordierite is a blue silicate mineral that occurs as crystals or granules in igneous rocks, it is composed of magnesium aluminum silicate

I. 2. 2 Cordierite properties

I. 2. 2. 1 Structural properties of cordierite:

There are three shapes of cordierite [4]

- ✓ α-Cordierite It is stable in high temperature and is common in nature, crystallizes in the hexagonal crystal system, with the lattice parameters a = 9.769 Å and c = 9.337 Å .
- ✓ β-cordierite Stable forms hydrothermally below 830°C.
- ✓ The equilibrium inversion temperature of β→α cordierite is given by Yoder as 830°C.
- ✓ μ-Cordierite found by Rankin and Merwin, forms metastably by crystallization of glass in air below 900°C, and then reverts somewhat sluggishly to the α form when heated above this temperature.

μ-Cordierite has been found to be structurally analogous to β-spodumene.

I. 2. 2. 2 phase diagram of Cordierite

The MgO-Al2O3-SiO2 system contains a number of ceramic materials, some of which can be adapted for special ceramics. The Cordierite secretion area is specific in the diagram shown in figure (I.1). In the so-called cordierite point, the mineral composition is $2MgO.2Al_2O_3.5SiO_2$. Cordierite stability range covers temperature range from 1465 to 1355°C. The last temperature corresponds to the lowest melting point in the system, which theoretically limits the maximum heat field for pure cordierite application [5].

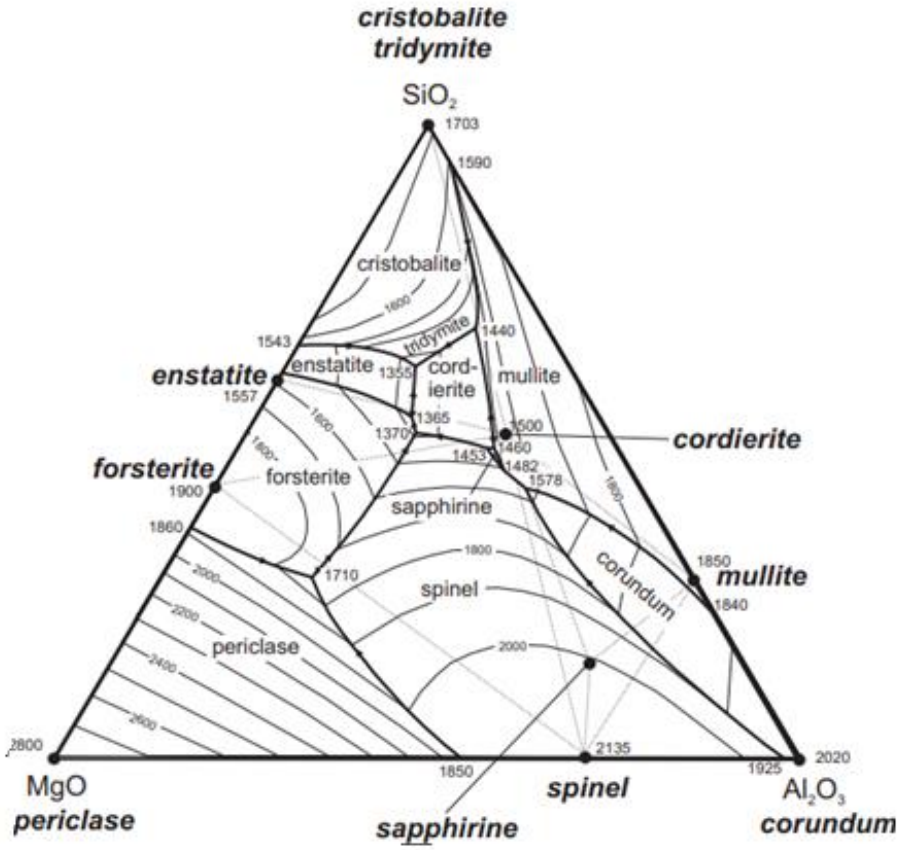

Figure (I. 1) Phase diagram Al_2O_3 - MgO - SiO_2 [5]

I. 2. 2. 3 Overview of Physical Properties

Cordierite has good thermal shock resistance and high dielectric strength, as well as low thermal expansion and low thermal conductivity [6], and some of the physical, mechanical, thermal and electrical properties are listed in the table (I.1).

Table (I.1) Cordierite properties [7. 8].

	properties	The value	Symbol
Physical properties	Density (g/cm3)	2 .58 - 2.66	ρ
	The maximum air temperature (°C)	1100	T
	Hardness (on Mohs scale)	7 - 7.5	
Mechanical properties	Young's modulus (GPa)	70	E
	Modulus of Rupture (MPa)	117	
	Poisson coefficient	0.26	U
	Bending resistance (MPa)	80-150	**σf**
	Durability (MPa.m1 / 2)	1 - 2	Kic
Electrical properties	Dielectric constant at 1MHz	5	εr
	Electrical resistivity at 20 °C (Ohm.cm)	10^{11} - 10^{14}	**σ**
	Insulation resistance (kV/mm)	5 - 15	
Thermal properties	Specific temperature (J/Kg K°)	900	Cp
	Thermal conductivity (W/m K°)	2.5	**σ**
	Thermal expansion coefficient (10^{-6}/K)	2 - 3	α
	Max. Operating temperature	1470 °C	T

I. 2. 3 Cordierite applications

Cordierite is widely used in various fields of ceramics. Its traditional applications are as follows:

- Aerospace applications and Cordierite astronomy (CO720) ceramic structural parts in a satellite based on Kyocera research [9] and a Subaru Telescope Viewfinder Separator. Electro-ceramics (resistors, fuses, flame guards, etc...) .
- Cordierite Coatings and Glasses and Making thick films.
- Cordierite substrates and filters. In the field of electrical insulation of resistors, burner tubes or firing supports in the ceramic industry [9].
- Production of prototypes, mounting molds and sensors.

I. 2. 4 Methods for preparing the cordierite compound

Cordierite has physical, mechanical and thermal resistance, and due to its absence in nature, researchers have prepared it in several ways to obtain a good sintering and at the same time preserve its properties, among which are three famous methods.

I. 2. 4. 1 The method of glass ceramics

It is characterized by microscopic crystals with homogeneous distribution that are formed by the old method of glass and then put in a moderate temperature until it crystallizes and in the end we obtain materials with glass properties and with homogeneous microscopic crystals and a very small percentage of voids.

I. 2. 4. 2 Method of raw materials in the solid state

The method is based on sintering pure oxides of MgO, Al_2O_3 and SiO_2 in proportions equivalent to the chemical composition of Cordite [10. 11], and because it is expensive, the researchers used inexpensive and naturally available raw materials such as clay and kaolin [12. 13] where the raw materials are mixed with the compound magnesium oxide MgO. It is then heat treated in proportions close to the chemical composition of cordierite [14].

I. 2. 4. 3 Sol-gel method

It is one of the methods extracted from wet chemistry techniques whose principle revolves around a set of water and condensation reactions at constant temperatures by dissolving powders of raw materials in a solution that often forms alcoholic oxides to form a sol solution, and after the water separates from it, it becomes a gel that is dried and condensed by heat treatment And we get the material to be obtained [15].

I. 3 Mullite

I. 3. 1 Definition of ceramic mullite

In the Al_2O_3 - SiO_2 system, the properties of mullite ceramics can be specially adjusted by changing the chemical and mineralogical composition. Pure mullite ($3Al_2O_3.2SiO_2$) usually consists of 82.7 % Al_2O_3 and 17.3% SiO_2. With the traditional sintering method, mullite ceramics are composed of a structure of mullite, aluminum oxide (Al_2O_3) and glass (SiO_2) mineral phases. Sintered mullite usually contains up to 10% of the vitreous phase – It has two stoichiometric forms: $3Al_2O_3.2SiO_2$ or $2Al_2O_3$. SiO_2. Natural mullite is rare in nature. It is named after one of the few known deposits on Mill Island [16], figure (I.2) represents phase diagram of the $SiO_2 – Al_2O_3$ system.

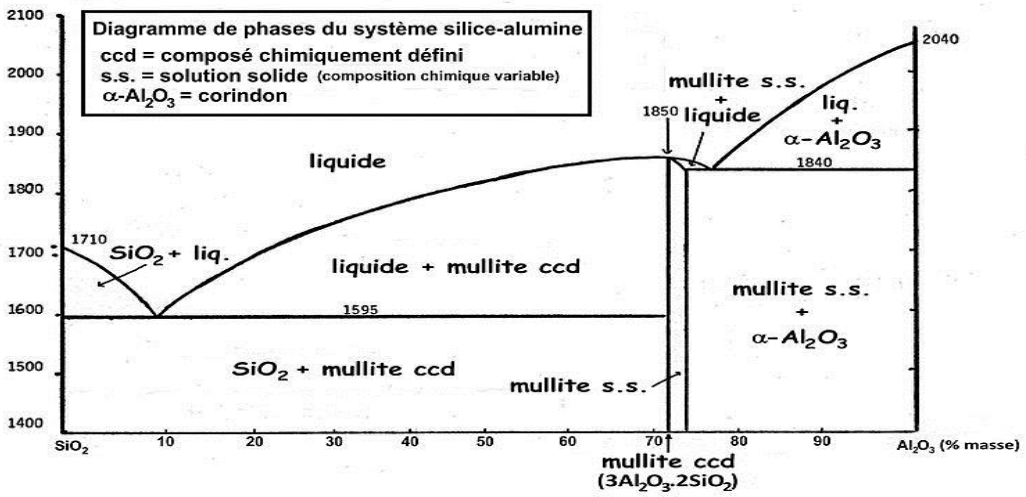

Figure (I. 2) represents phase diagram of the $SiO_2 – Al_2O_3$ system [16. 17].

I. 3. 2 Crystal Structure of Mullite

The crystal structure of mullite (nominally $3Al_2O_3.2SiO_2$) is orthorhombic with the space group Pbam and unit cell dimensions a = 0.7540 nm, b = 0.7680 nm and c = 0.2885 nm for the stoichiometric composition (Angel and Prewitt, 1986). An [001] projection of an ideal unit cell is shown in Fig. (I. 3), from which it can be seen that mullite consists of chains of AlO_6 octahedra at the edges and centre of the unit cell, running parallel to the c-axis. These chains are joined by $(Al,Si)O_4$ tetrahedra forming double chains, which also run parallel to the c-axis (nm) [18- 20].

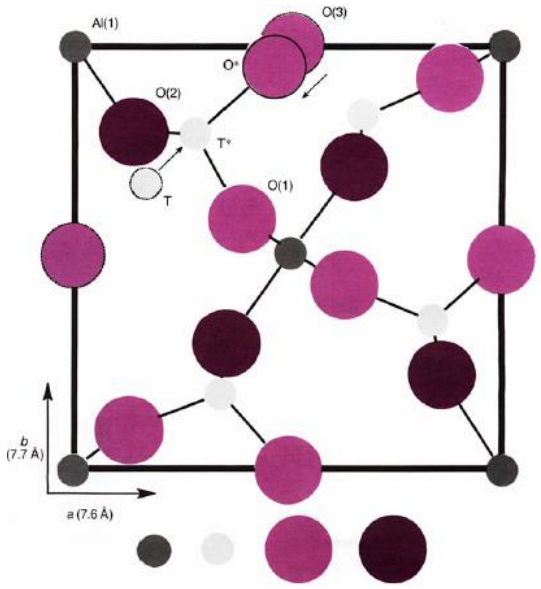

Figure (I. 3) Projection along [001] direction of the ideal unit cell of mullite showing T to T* transition of the cations (indicated by an arrow) following the formation of oxygen vacancy (large dotted circle) and readjustment of oxygen in the O(3) positions. [18]

I. 3. 3 Mullite properties

Mullite is an excellent structural material due to its high temperature stability, strength and creep resistance. Hence many characteristics as shown in the table (I.2).

Table (I. 2) Mullite properties [21. 22].

	properties	The value	unit
Physical properties	Density	**3.03**	**g/cm3**
	Max. Use Temperature (* denotes inert atm.)	**1700**	**°C**
Mechanical properties	Hardness	**1450**	**knoop (kg/mm^2)**
	Compressive Strength	**551**	**MPa**
	Young modulus	**130**	**GPa**
	Stress intensity factor	**2 - 4**	**MPa.m-1/2**
	Modulus of rupture	**160**	**MPa**
	Poisson's Ratio, υ	**0.25**	
	Fracture Toughness, K_{Ic}	**2.0**	**MPa x m$^{1/2}$**
Electrical properties	Dielectric Constant at 1MHz.	**6.0**	
	Dielectric Strength	**9.8**	**kV/mm**
	Electrical Resistivity	**10^{13}**	**Ωcm**
Thermal properties	Thermal Shock Resistance	**300**	**ΔT (°C)**
	Coefficient of Linear Thermal Expansion, α_l	**5.3**	**µm/m-°C (~25°C through ±1000°C)**
	Specific Heat, c_p	**0.23**	**cal/g-°C**
	Coefficient of thermal expansion	**4.5 - 5.6. 10^{-6}**	**1/°C**
	Thermal conductivity **(100 -1400 ° C)**	**4.0-6.0**	**W / m.K**

I. 3. 4 Mullite applications

Mullite is of increasing importance in electronic and optical structural applications and high temperatures, due to its low dielectric stability, good infrared transparency and excellent creep resistance. Classical uses of mullite contain refractories in

- Hot metal mixers and low-frequency induction furnaces, as well as plates and columns for preparing furnaces for firing ceramic tools.
- Protective coatings and mullite insulators for corrosion resistance for corrosive industrial environments by air plasma spraying (APS) methods.
- Turbine engine components.
- Infrared transparent window for use in high temperatures [21].

- Monolithic mullite porcelain (filters, catalyst support substrates and electronic devices with high temperature stability and high electrical resistance).
- Casings for heat pairs and heat exchangers.
- Mullite matrix composites (heat shields in the aerospace industry).
- Mullite fiber (reinforced for glass and ceramic glass) [22].

I. 3. 5 Mullite preparations from sol-gel

Sol-Gel Method There has been considerable interest in preparing mullite from chemically synthesized precursors. In particular, sol-gel methods have been widely used to produce mullite powders, fibers, and bulk samples at relatively low processing temperatures. In sol-gel treatment, the colloidal or suspended particles, sol, undergo a chemical change that causes them to be bound together in a continuous network called a gel. The sol-gel method allows the preparation of a homogeneous and reactive gel which can be sintered at a low temperature. A reaction in this way is basically the same as the reaction that occurs with a mixed solid, if the materials are mixed under wet conditions. However, the particle size varies greatly for the two methods of preparation. SOLs (nanometers) are much smaller than those used in the traditional method (micrometers), using the correct bonds of silica soles and alumina to intelligently form mullite, prepare the alumina solution by dispersing beta alumina particles in the hydrochloric acid solution. Then slowly add silica sol to this suspension and adjust it to pH 6-7, in this pH range, the surfaces of alumina particles are positively charged while the silica particles are negatively charged. Therefore, heterogeneity can be expected, and from it homogeneous mixing and obtaining a colloidal solution [20]. Figure (I.4) represents an example of the method.

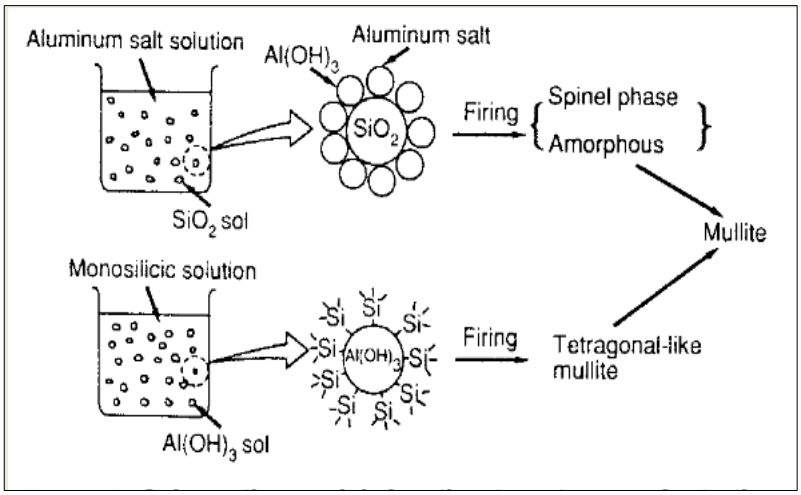

Figure (I. 4) Schematic model for the two types of starting material for a mixture of sol and salt [20].

I. 4 Cordierite – mullite composites

I. 4. 1 Definition of cordierite – mullite composites

Cordierite and mullite are the main technical ceramics in the ternary oxide system MgO-Al_2O_3-SiO_2 with versatile potentialities of applications. Ceramics materials based on cordierite-mullite composite are of great importance as refractory and other technical ceramic materials due to their low thermal expansion coefficient, excellent thermal shock resistance, low dielectric constant, high refractoriness and high mechanical strength [23].

I. 4. 2 Properties of cordierite-mullite composites

Properties making it useable in various applications are:

- The composition has a longer service life and excellent thermal shock resistance.
- Light volume, high thermal stability, thermal expansion and low conductivity.
- Improved creep resistance at high temperature, energy saving effect.
- Cordierite has high bending strength due to low thermal expansion and low sintering range, and the presence of mullite helps to expand the sintering range, and increase the resistance of refractory materials.
- Mullite has higher operating temperature than Cordierite but as a compound, its maximum operating temperature is -1350 ° C [24].

I. 4. 3 Applications of cordierite-mullite composites

Composite cordierite- mullite are used as:

- Ceramic filter and as thermal shock resistant material.
- Ceramic electrode, integrated circuit substrate.
- pillars catalytic converter to control exhaust gas in cars
- Gas turbine motor heat exchanger, industrial furnaces.
- Packaging materials in electronic packaging.
- Metal refractory coating.[25]

I. 4. 4 Preparation of mullite - cordierite with Sol Gel

Compound mullite / cordierite powders containing different proportions of cordierite were prepared by a sol-gel method using bohemite, colloidal silica, and $Mg(NO_3)_2\ 6H_2O$. Mullite and cordierite sols were prepared separately and mixed to form the sol complex. The mullite

temperature depends on the cordierite content in the compound. Also, α-cordierite crystallizes at a low temperature in a compound rich in mullite (MC20) [26].

I. 5 Calculation of activation energy

1. 5. 1 Calculation of activation energy

There are several approximate methods suggested by researchers on how to calculate activation energy, which is the energy required to form one mole of any phase. These methods differ according to their nature and conditions, and one of the most important conditions is the treatment temperature, so we find:

1. 5. 1. 1 Case isothermal

It is based on differential thermal analysis DTA and theory Johnson–Mehl–Avrami

We find the equation

$$x = 1 - \exp((-kt)^n) \text{ ..... (1)}$$

$$K = K_0 \exp(-\frac{E_a}{RT}) \text{ ..... (2)}$$

Whereas

X: percentage of crystallization.

K: the speed constant of the reaction and depends on the temperature according to a relationship Arrhenius.

E_a: Activation energy. T: temperature (k°). R: the ideal gas constant. n: Avrami exponent.

K_0: Atomic oscillation coefficient.

When entering the logarithm twice in the relation (1), the value of k and n can be set by plotting the data of changes in terms of time, and after setting k, $E_a$can be calculated; And also K_0, by entering the logarithm in equation (2) by plotting the changes in terms of (1 / T) Based on (1 and 2), the velocity of crystallization can be found by the following equation:

$$(\frac{dx}{dt}) = kf(x) = k_0 \exp(\frac{E_a}{RT}) f(x] \text{.....(3)}$$

And by inserting the logarithm into equation 3, we find:

$$\text{Ln}\,(\frac{dx}{dt}) = \ln\left(k_0 n(1-n)^{\frac{n-1}{n}}\right)(1-n) - \frac{E_a}{RT} = \text{Ln}\big(k_0 f(x)\big) - \frac{E_a}{RT} \quad \text{[27]..... (4)}$$

Legero and his group also proposed a mathematical method based on the results of non-static experiments by choosing a set of crystallization ratios and different heating speeds. Depending on equation (3), it is possible to calculate n and take the crystallization ratios x_1 and x_2, which meet the following conditions:

$$\text{Ln}\big(k_0 f(x_1)\big) = \text{Ln}\big(k_0 f(x_2)\big)$$

$$\text{Ln}\,(1\text{-}x_1)+\frac{n-1}{n}\,\text{Ln}[-\,\text{Ln}(1\text{-}x_1)]=\text{Ln}(1\text{-}x_2)+\frac{n-1}{n}\,\text{Ln}[-\,\text{Ln}(1\text{-}x_2)] \quad \ldots\ldots\ldots\ldots(5)$$

And n can be calculated as follows

$$n=\frac{\ln(\frac{\text{Ln}(1-X2)}{\text{Ln}(1-X1)}}{\ln[\frac{(1-X2)\ \text{Ln}(1-X2)}{(1-X1)\ \text{Ln}(1-X1)}]} \quad [28]\ldots\ldots\ldots\ldots\ldots\ldots\ldots\ldots\ (6)$$

1. 5. 1. 2 Case non-isothermal

$$T=\ T_0\ \int \emptyset dt \quad \ldots\ldots\ldots\ldots\ (7)$$

Whereas T: temperature , T_0 Initial temperature, $\emptyset=\frac{dT}{dt}$ heating speed

Substituting equation (7) into equation (5), we find

$$x=1-\exp(-\left(k\frac{(T-T_0}{\emptyset}\right)^n) \quad \ldots\ldots\ldots\ldots\ (8)$$

And from it the speed of crystallization

$$\frac{dx}{dt}=(\frac{\partial x}{\partial t})_T+(\frac{\partial x}{\partial T})_t(\frac{dT}{dt}\ ) \quad \ldots\ldots\ldots\ldots\ldots\ldots\ (9)$$

Constant time means that the number of sites of the particles is fixed, and from that the speed of crystallization become

$$\frac{dx}{dt}=k_0\ (1-x)\ \exp(-\frac{E}{RT}) \quad \ldots\ldots\ldots\ldots\ldots\ (10)$$

The speed of crystallization is maximum at T_m $\Longrightarrow$ $\frac{d^2x}{dt^2}=0$ $\ldots\ldots\ldots\ldots\ldots\ldots$ (11)

$$\frac{E}{RT_p{}^2}(\frac{dT}{dt})=k_0\exp\,(-\frac{E}{RT_p}) \quad \ldots\ldots\ldots\ldots..(12)$$

After simplifying and modifying the equation (12), the researcher Kissinger reached

$$\text{Ln}\,(\frac{\varphi}{T_p{}^2})=-\frac{E}{RT_p}+(con) \quad \ldots\ldots\ldots\ldots\ldots\ (13)$$

Matusita and coworkers [27] have proposed a modified form of the Kissinger equation as:

$$\text{Ln}\,(\frac{\varphi^n}{T_p{}^2})=-\frac{m\,E}{RT_p}+(con\ 1) \quad \ldots\ldots\ldots\ldots\ (14)$$

m: Scalar operator which determines mechanism growth Granules

Calculation of activation energy by the Ozawa method:

$$\text{Ln}\,(\varphi)=-\,1.0518\frac{E_a}{RT_p}+C_1 \quad [29]\ldots\ldots\ldots\ldots\ (15)$$

Or the Boswell method

$$\text{Ln}\,(\frac{\varphi}{T_p})=-\frac{E}{RT_p}+C_2 \quad [30]\ldots\ldots\ldots\ldots\ (16)$$

CHAPTER II

Experimental methods used and devices used

In this chapter, we will talk about the raw materials used and the experimental methods used, as well as some methods of analysis and measurement, and the most important devices used.

II. Experimental methods used and devices used

II. 1 The Used Materials

In the study we used several raw materials, represented in Figure (II.1):

1. Magnesium nitrate hexahydrate $Mg(NO_3)_2 \cdot 6H_2O$.
2. Aluminum nitrate nonahydrate $Al(NO_3)_3 \cdot 9H_2O$.
3. TEOS (formally namedtetraethyl orthosilicate) $Si(C_2H_5O)_4$.
4. Ethanol (C_2H_5OH).

In addition to the use of other laboratory means

Figure (II.1) : The raw materials used.

II. 2 Experimental methods

II. 2 .1 Method for preparing the cordierite-mullite composite by the sol-gel method

1. Weigh an amount of aluminum nitrate and magnesium nitrate powders on an electronic scale, then add to them a certain amount of solvents which are water and TEOS to get two solutions.
2. Mix the two solutions separately using a magnetic mixer.
3. The remaining TEOS are added and ethanol.
4. Mix all solutions together in a magnetic mixer for 2 hours at room temperature 25 ° C until the solution becomes transparent.
5. The solution was then placed in a 60 ° C oven for 48 hours.
6. Gel is formed.

7. Put the gel in another oven at 120 ° C for 24 hours.
8. With grinding, we obtain cordierite-mullite powder in a certain proportion.

Table (II.1) Represents the quantities of raw materials to obtain cordierite mullite composite proportions.

	M(NAl) (g)	M(NMg) (g)	M(TEOS) (g)	V H_2O (ml)	V Ethanol (ml)
M100C00	13.3496	0	2.4967	53.5208	9.9870
M95C05	13.0062	0.1108	2.5992	55.7176	10.3969
M50C50	9.9159	1.1079	3.5215	75.4883	14.0861
M00C100	6.4822	2.2158	4.5463	97.4557	18.1852

II. 2. 2 Formation of samples

To study samples in Dilatometric, we need to press a powder from pre-prepared powders into a mold of treated steel using a manual hydrostatic press with a maximum mass of 12 tons, but in the pressing process we used 1 ton and a mass = 500 mg for 4 minutes to obtain a sample with a fixed diameter (d = 13 mm).

II. 2. 3 Sintering of samples

In order to study the calcined samples, we introduced one of the samples into an oven at 700 ° C for two hours (To get rid of nitrates, water, etc.) then we shape it for Dilatometric study.

II. 2. 4 Dilatometric Study

We used a DIL402C NETZSCH differential linear expansion apparatus with a maximum temperature of about 1600 ° C in order to know the phase transitions and study the kinetics of the treated material transformations. And by using the previous device, we heated samples to different temperatures (750, 1000, 1095, 1130, 1230, 1325 and 1400 °C), and we also heated M50C50 samples from room temperature to 1400 °C for different heating rates (3,5,7,9 and 11° C min^{-1}).

II. 2. 5 Differential Scanning Calorimet DSC and Thermogravimetric Analysis TGA

In order to determine the phase transformations that occurred during the heat treatment of Cordierite -Mullite powders, we perform DSC and TG experiments at different temperatures using a LABSYS EVO DTA / DSC-TG SETARAM instrument .

- ✓ M50C50 was heated at (1430 °C) at a constant heating rate of 30 ° C min^{-1} .

II. 2. 6 X-ray diffraction Analysis

After each heat treatment, Cordierite- mullite compound powder was analyzed by X-ray diffraction analysis, using a diffractometer. This technique enables us to know the different crystal stages that are forming. During a heat treatment using the information recorded on the diffraction spectrum, analyzing the resulting spectra gives us information about the phases of the phases in the sample.

II. 2. 7 FTIR Analysis:

Analysis of primary samples of XRD that we studied using FTIR-8300 to discover phases that did not appear amorphous by taking a quantity of a sample of corderite -mullite complex with addition of KBr.

II. 2. 7. 1 How to prepare an FTIR sample:

a) We put KBr in a 120 degree oven for two days to remove moisture.
b) We take 1 percent of the sample to be studied and the rest, or 99 percent KBr.
c) Combine in a small FTIR bowl, and crush for one minute.
d) We compress a small amount of the resulting powder by means of a manual hydraulic press with an air pump for 5 minutes with a force of 80,000 N.
e) We obtain a thin sample and place it in a special holder for studying with the device Figure (II.2)

Figure (II.2) A thin sample placed in a special holder for studying with the device and means of pressure.

II. 3 The Used Equipment:

II. 3. 1 Differential Thermal Analysis DTA, Differential Scanning Calorimet DSC and Thermogravimetric Analysis TGA

DTA: The DTA involves heating or cooling of a test sample and an inert reference in which the sample and the reference are placed symmetrically in the oven. The oven is controlled by a temperature program and the sample and reference temperatures are changed. During this process, a differential thermocouple is set up to detect the temperature difference between the sample and the reference. Also, the sample temperature is detected by the thermocouple on the sample side.

TGA: This method is based on measuring the amount of decrease or increase in the weight of the substance as a result of heating, and a device called thermo balance is used for this. The change in the mass of the sample is recorded in terms of temperature or time, and the resulting curve is called a thermogram. In this way, one or more components can be analyzed..

DSC is used to analyze compounds by measuring the amount of heat absorbed and emitted by those compounds .The basic principle in this method is to make the sample and the standard material at the same temperature by applying electric energy while heating or cooling them at a linear speed. The resulting curve expresses the relationship between heat flow.

Figure (II.3) Represents the device used.

Figure (II.3) LABSYS EVO DTA/DSC-TG SETARAM equipment.

II. 3. 2 Fourier Transform Infrared (FT-IR Spectrometer):

This device analyzes all types of samples, whether solid, liquid or gas, and to find out their molecular structure. By measuring the infrared radiation transmitted or absorbed by these samples, and measuring the concentration of many materials over a wide range of wavelength, including the visible light region and the ultraviolet region. A device was used FTIR-8300 SCSI Figure (II.4) .

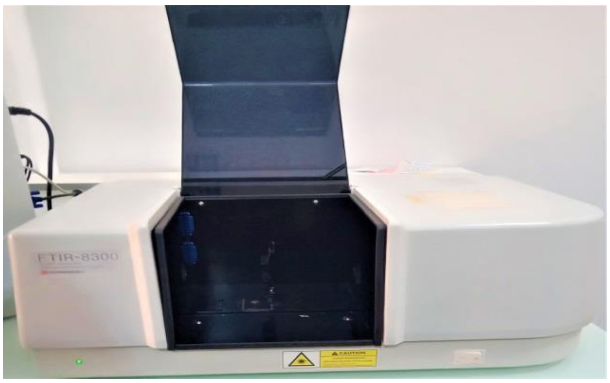

Figure (II.4) :FTIR-8300 SCSI

II. 3. 3 The Diffractometer:

To determine the formed phases of the heat treated powders, we analyzed them by means of an X-ray diffraction device of the diffractometer MRD, PANalytical (ISM) type with the use of CuKα radiation with a wavelength of 0.15418 nm as shown in Figure (II.5). It was used in this study based on the extrusion of samples using a monochromatic X-ray beam.

$2d_{hkl}\sin\alpha = n\lambda$

n : diffraction range, α: diffraction angle , λ: wavelength of X-rays and d_{hkl}: the dimension between crystalline levels.

Figure (II.5): a diffractometer MRD, PANalytical (ISM)

II. 3. 4 Dilatometer

we used equipment NETZSCH (Dil 402 C). The maximum temperature is 1600 ° C. The sample is placed in a special holder that contains a thermocouple that measures the temperature of the sample in an electric oven. When the sample is heated by a gradual change in temperature, a change in its dimensions occurs in order to know the phase shifts and study the kinetics of the transformations of the treated material, because X-rays do not give all the information, especially in the case of amorphous phases, and the linear expansion device is very sensitive to any A transformation takes place in matter, and it also helps us understand the phenomenon of sintering based on the contraction that occurs in matter. Usually in this device is used as standard, and we used aluminum oxide as standard Figure (II.6)

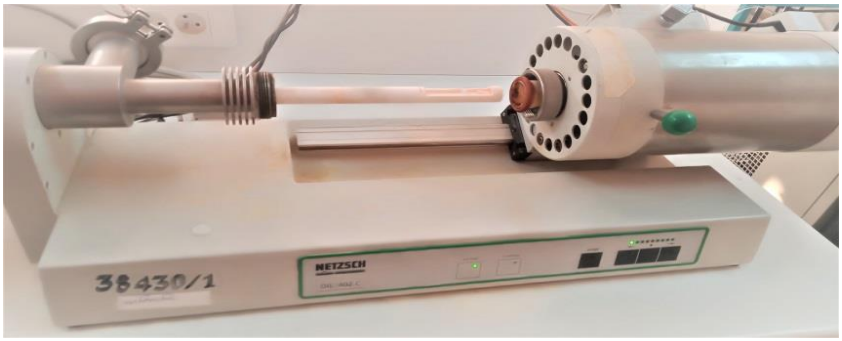

Figure (II.6): The type of "NETZSCH DIL402C" expansion scale.

II. 3. 5 Heat Treatment Furnace

Heat Treatment experiments were carried out using a nabertherm type furnace show in figure (II.7) where its maximum tempertaure could reatch 1300 °C and more.

Figure (II.7): "Naberthem" type furnace.

II. 3. 6 hydraulic press

Manual hydraulic press for delatometric samples maximum mass 12 ton, and hydraulic press for FTIR samples get to 80 KN show in Figure (II.8)

Figure (II.8): hydraulic press

II. 3. 7 Magnetic mixer:

It is used for mixing solutions and the mixing speed can be controlled. We use speed 5 , the device used is of type Agmatic n Figure (II.9).

Figure (II.9): Magnetic mixer Agmatic n.

II. 3. 8 Electromagnetic balance:

For use in weighing raw materials and the rest of samples Type of aeADAM Nimbus Figure (II.10).

Figure (II.10): Electromagnetic balance aeADAM Nimbus .

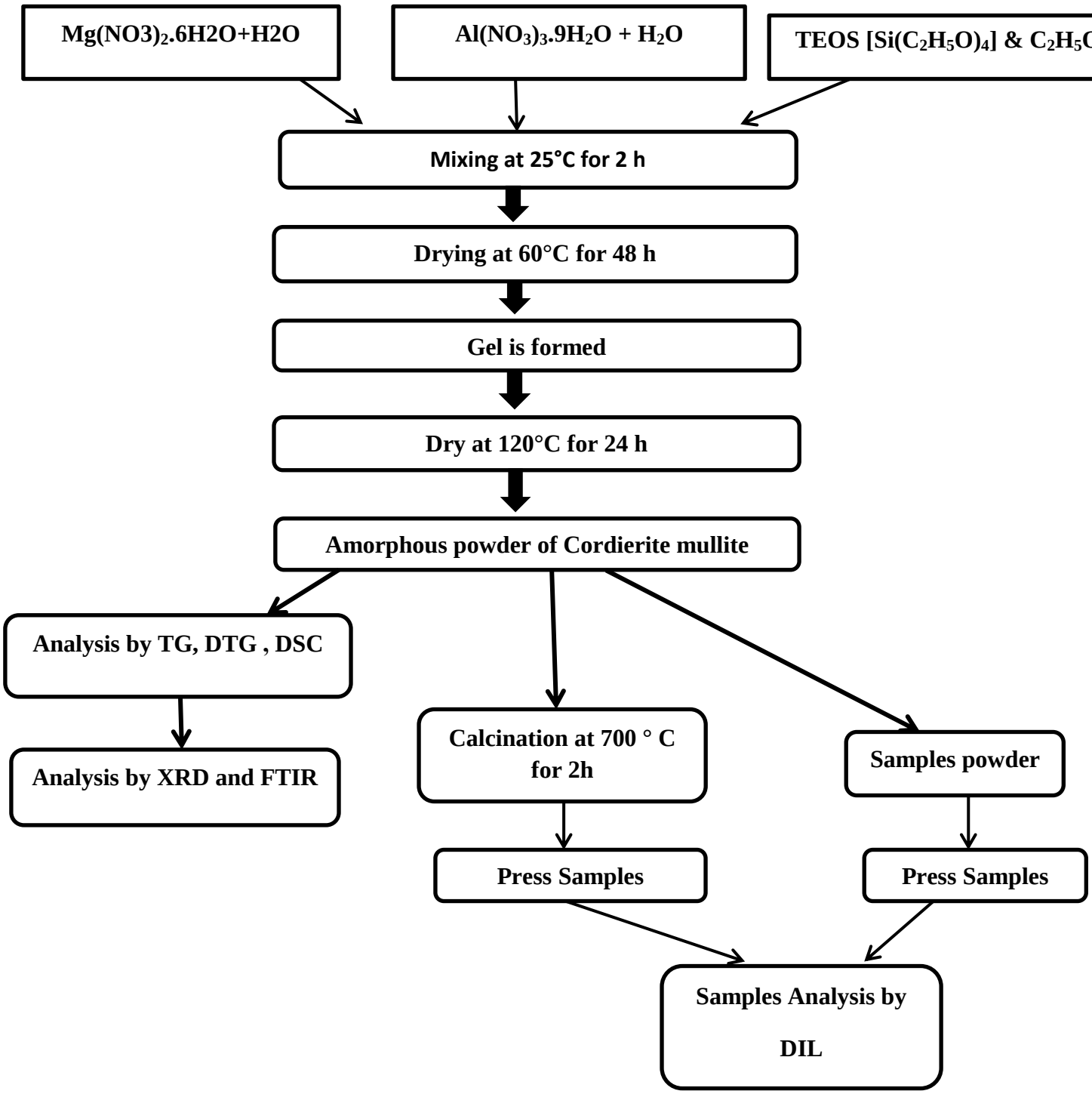

Figure (II.11) Flowchart to experimentally study the Cordierite mullite composite.

Chapter III

Experimental results and discussion

In this chapter, we deal with the experimental results that we obtained in the first stage. We analyzed the cordierite - mullite compound using thermal gravimetric analysis (TGA) as well as the Differential Scanning Calorimetry (DSC) in the second stage we carried out a Dilatometric study of the compound in the third phase we used the X-ray diffraction device and discussed the results of X-rays then we moved on to an analytical study using the Fourier device to convert the infrared spectrum and in the end the calculation of the activation energy of the cordierite and spinel.

III.1Thermal study

III.1.1. Thermo gravimetric analysis (TGA)

The figure (III.1) represent the mass loss and it first derivation (TG/DTG) curves of mixture M50C50 treated from room temperature to 1000 °C, at heating rate of 30 °C/min.

The TG/ DTG curve shows:

- ✧ Only one weight loss occurred between 100 °C to 700 °C and it is probably attributed to the existed three intervals (endothermic peaks).
- ✧ The first mass loss in the temperature range 100 – 220 °C is due to the release of water adsorbed on the surface of the particles (dehydration) corresponding entirely to the first endothermic peak at 181 °C.
- ✧ The second mass loss in the temperature range 250–350 °C is due to the decomposition of nitrate (aluminum nitrate and magnesium nitrate), correlating with the second endothermic peak at 295.24 °C.
- ✧ The third mass loss in the temperature range 350–500 °C is due to the decomposition of TEOS and combustion of organic matter [31, 32], correlating with the third endothermic peak at 382 °C.

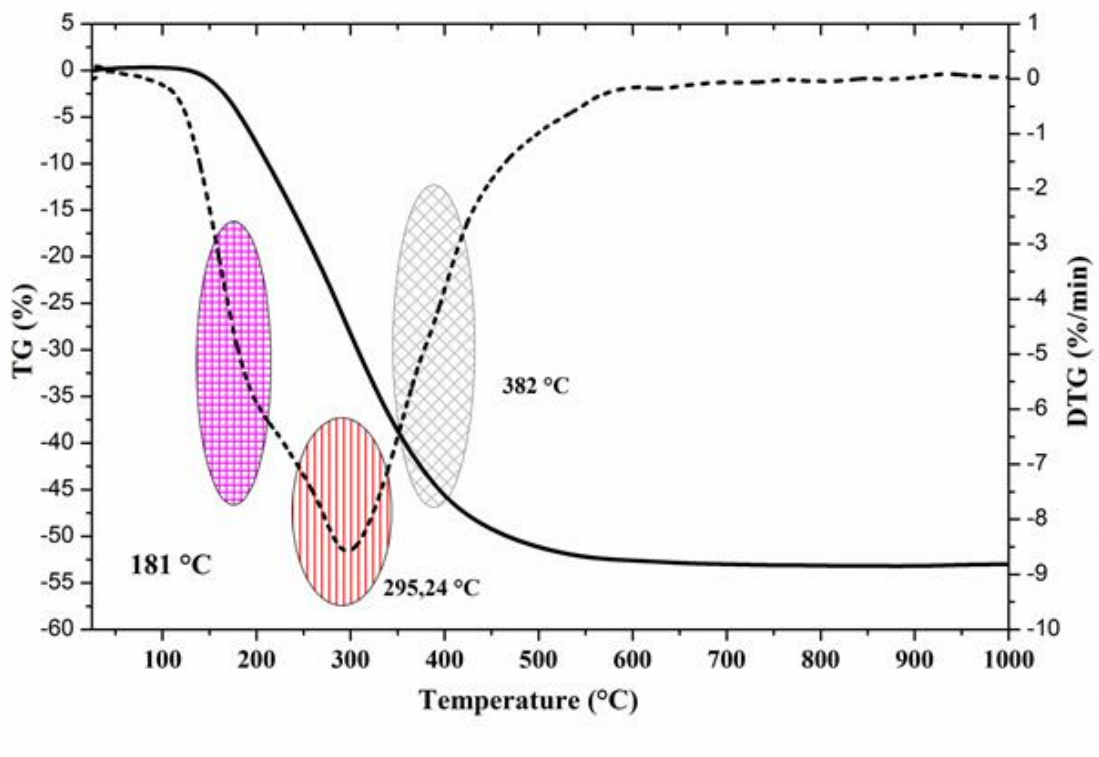

Figure (III.1) TG/ DTG curves of mixture M50C50 at heating rate of 30°C/min.

III.1.2 Differential Scanning Calorimet DSC

Figure (III.2) shows the typical DSC curve of M50C50 treated from room temperature to 1400°C with heating rate 30 °C/min, it is indicating the presence of three endothermic peaks, and four exothermic peaks in the temperature range of 700 to 1420 °C.

- ✧ The first exothermal peak at temperature 955.6 °C can be assigned to the formation of Al-Si spinel phase.
- ✧ The second exothermal peak almost at 1135 °C is associated to the formation of mullite phase.
- ✧ The third exothermal peak approximately at 1236 °C is properly related to μ-cordierite phase formation.
- ✧ The last exothermal peak approximately at 1352 °C is related to α-cordierite phase formation [33, 34].

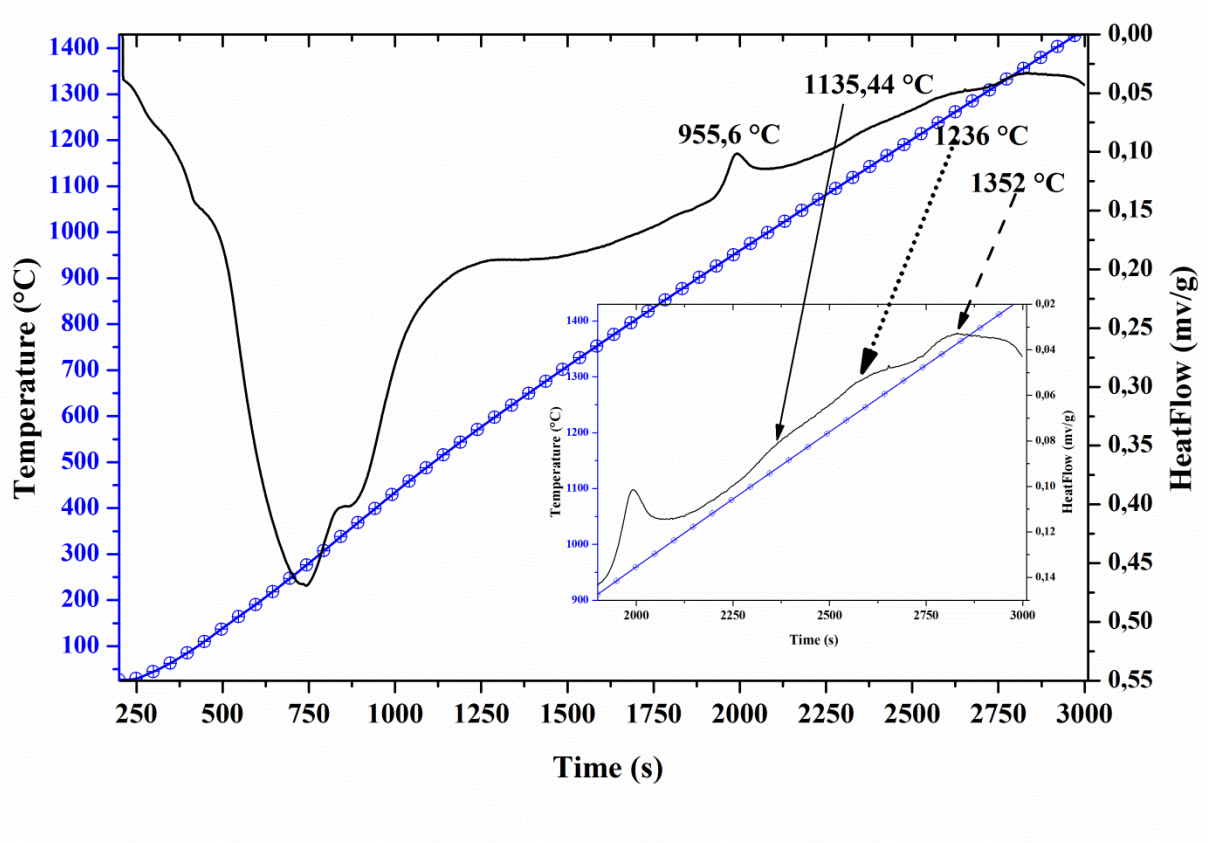

Figure (III.2) The DSC curves of M50C50 powder heated at 30 °C/min.

III. 2 Dilatometric study

Figure (III.3) shows a typical linear shrinkage curve and its first derivative for M50C50 mixture treated at heating rate of 05 °C/min. It can be clearly seen that there are four transformations. The first transformation is a relative linear shrinkage which starts at 718 °C and ends at 994°C where the rate of shrinkage is maximum at 882.95 °C; this shrinkage is due to the formation of spinel (Al-Si) and and the maximum shrinkage rate is about 10.43 %.

The second transformation is a third relative linear shrinkage that corresponds to the change of spinel to mullite phases at a temperature of 1075.80 °C and this transformation ends at a temperature lower that 1200°C. The third transformation is a relative linear shrinkage which starts at 1216 °C and ends at 1270 °C where the rate of shrinkage is maximum at 1242 °C; this shrinkage is due to the formation of μ-cordierite. The fourth transformation is a last relative linear shrinkage which starts at 1247 °C and ends at 1386 °C where the rate of shrinkage is maximum at 1274 °C; this shrinkage is due to the transformation of μ-cordierite to α-cordierite.

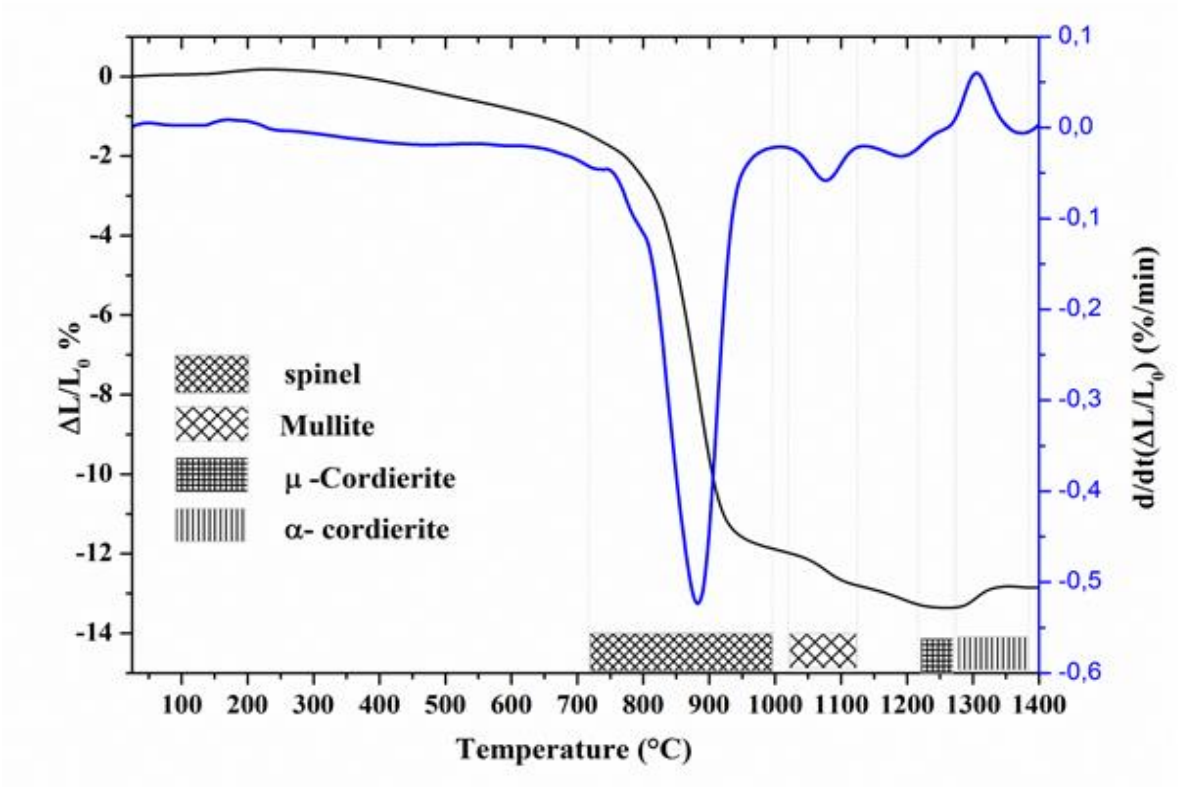

Figure (III.3) Relative linear shrinkage curve and its first derivative for mixture M50C50 treated at heating rate of 05 °C/min

Figures (III.4) and (III.5) shows a typical linear shrinkage curve and its first derivative respectively for M50C50 mixture that have been treated in several temperatures (750, 1000, 1130, 1230, 1325and 1400 °C), at heating rate 30 °C/min:

- In the 750 °C curve, there is no shrinkage appearing at this temperature, and all phases remain amorphous according to XRD results.
- A first linear shrinkage appears in the 1000 °C, and it is associated with the formation of the spinel phase (Al-Si) and (Al-Mg).
- The 1130°C curve indicates to the start of mullite phase formation which is confirmed by XRD results.
- At 1230 °C the emergence of a new linear shrinkage of approximately 0.92 % associated with μ-cordierite formation.
- At 1325, the last linear shrinkage starts at 1278 ° C and ends at 1323 °C, this shift results in an increase in size and elongation of about 0.23 %, with a maximum shrinkage rate of 1307 ° C, which is related to α-cordierite phase formation.
- The last curve treated at 1400 °C indicates a fully formed linear shrinkage that was related to α-cordierite phase.

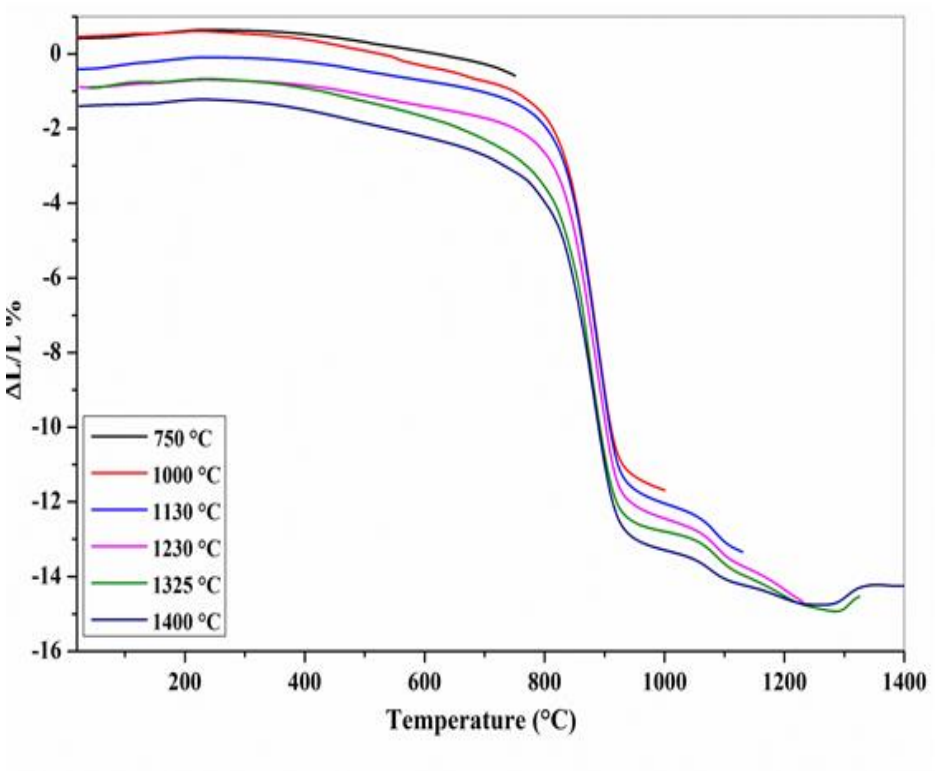

Figure (III.4) relative linear shrinkage curves for mixture M50C50 treated at heating rate of 05 °C/min.

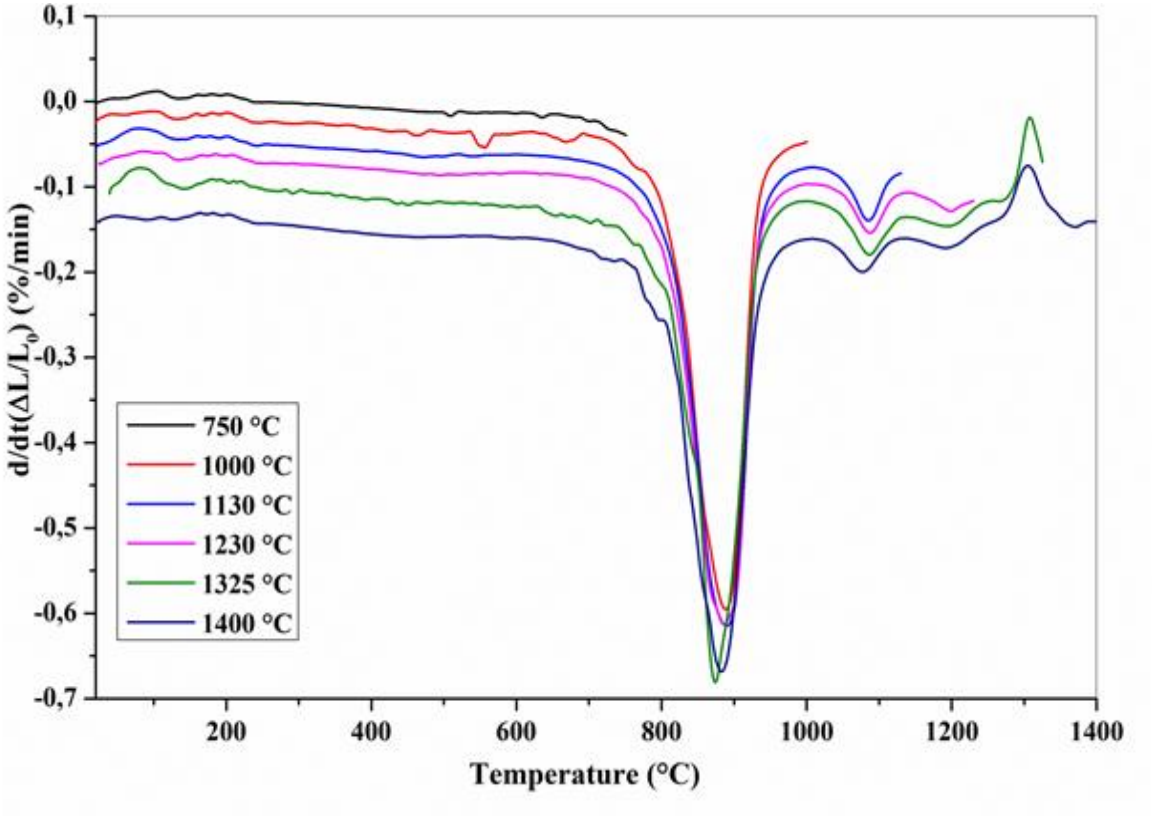

Figure (III.5) Curves of first derivative for mixture M50C50 treated at heating rate of 05 °C/min.

III. 3 X-ray diffraction Analysis

In order to determine the nature of all processes corresponding to the dilatometry , and to characterize all crystalline substances that formed during heating treatment, a M50C50 samples were treated in range of temperatures form 25 °C to 1400 °C, at heating rate 30 °C/min, then have been studied by X-ray diffraction (presented in Figure (III.6)) . It shows the following:

- ✧ The powders remain amorphous up to 750 ° C.
- ✧ At 1000 ° C Al-Si spinel appears and part of it turns into a semi-mullite, and while increasing treatment temperature to 1130 °C, Al-Si spinel phase disappear and mullite phase start forming, and the Mg-Al spinel appeared with more peaks.
- ✧ Both μ-cordierite and α-cordierite phase appear at 1230 °C along with decreasing in Mg-Al peaks.
- ✧ All mullite phase peaks are fully appeared at 1325 °C and μ-cordierite phase was transformed to α-cordierite completely.

- ✧ At 1400 °C, the Mg-Al spinel phase disappeared, and only mullite and α-cordierite phase was remained [23, 33, 35-39].

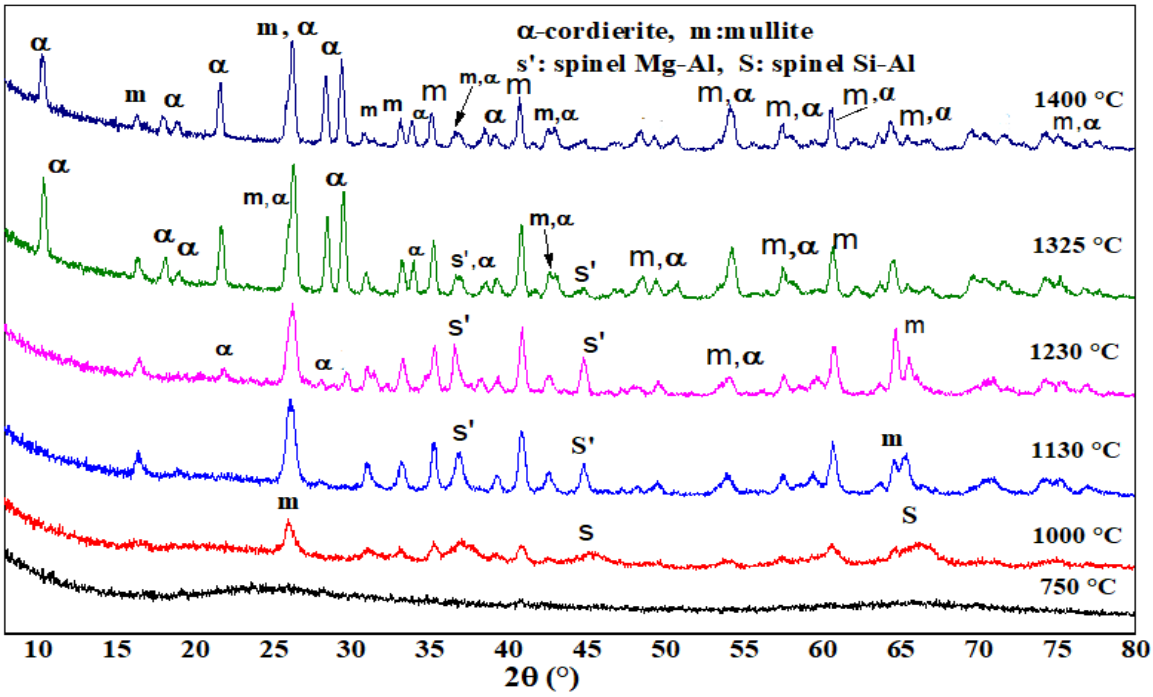

Figure (III.6) XRD patterns of mixture M50C50 treated at different temperature by dilatometry for heating rate of 05°C/min.

III. 4 FTIR Analysis

In order to identify all chemical compositions and bonds, a M50C50 powders that have been treated at 1400 °C by dilatometry. The results of FTIR spectroscopy of M50C50 composite obtained by Dilatometry treatment are illustrated in Figure (III.7), shows:

- ➢ Impulses from 2341 cm^{-1} to 2426 cm^{-1} express the distinctive signature of pulse at 1631 cm^{-1} is H_2O bending vibration.
- ➢ The characteristic vibration at 1384 cm^{-1} indicates NO_3^- bonds in the gel structure, the pulse represents at 1154.59 cm^{-1} belongs to Si-O-Si and the pulse at 956 cm^{-1} for SiO_4 structure (tetrahedral cordierite in the composite)
- ➢ The tetrahedral coordination gives the expansion of the Al-O bond in the two pulses 828 cm^{-1} and the 825.68 cm^{-1} distinctive and the very small pulse at 819 cm^{-1} represents SiO_4.
- ➢ The pulse found at 767.23 cm^{-1} corresponds to Si-O-Si vibration and pulse at 666 cm^{-1} he is Al-O vibration.

- The pulse at 578 cm^{-1} has been assigned to the vibrations of MgO or Al-O stretch (AlO_6) [38, 40- 43].

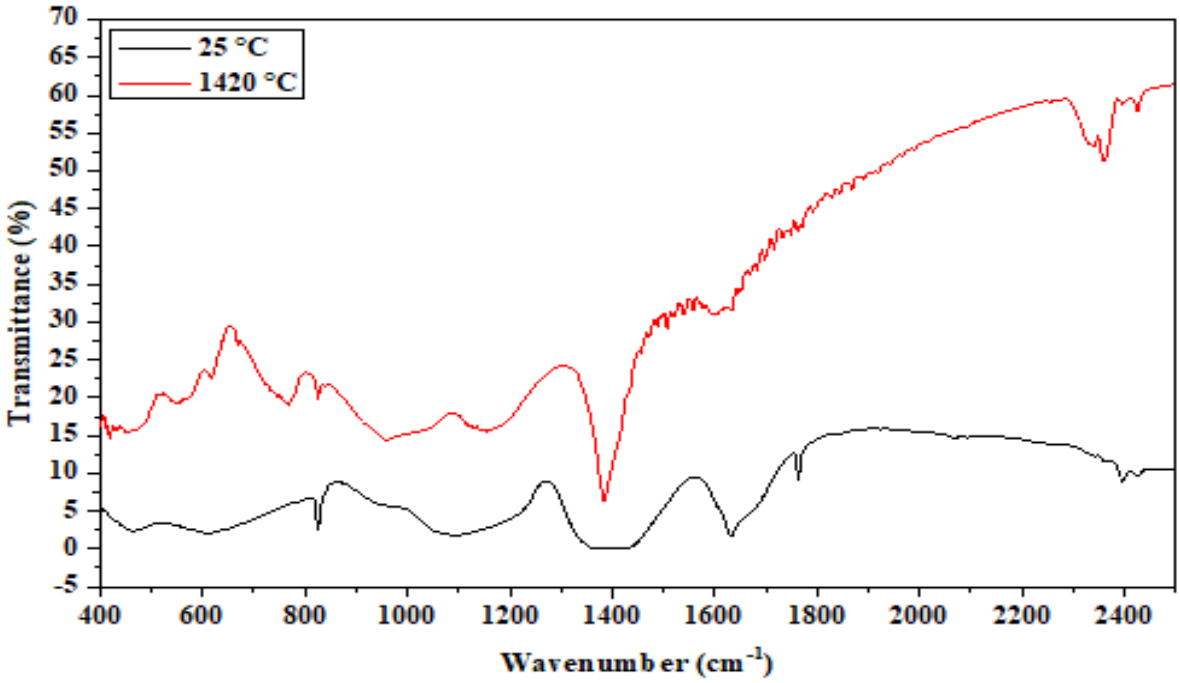

Figure (III.7) IR spectra of rnullite-cordierite composite (M50C50) gel powders.

III. 5 Activation Energy

III. 5 .1 Non-isothermal treatment

III. 5 .1. 1 Activation energy of cordierite formation using dilatometer

The linear relative shrinkage curves as function of temperature at heating rates of 3, 5, 7, 9, and 11°C/min were used to calculate the activation energy for the formation of the different phases following the Kissinger and Ozawa equations.

Ozawa equation: $\ln(\varphi) = -1.0518\frac{E_a}{RT_p} + c$ …… (1)

Boswell equation: $\ln\left(\frac{\varphi}{T_p}\right) = -\frac{E_a}{RT_p} + c$ ……. (2)

Kissinger equation: $\ln\left(\frac{\varphi}{T_p^2}\right) = -\frac{E_a}{RT_p} + c$ …… (3)

The maximum temperature (Tp), at different heating rates, for the formation of cordierite, Figure (III.8) was obtained from the derivative of the linear shrinkage curve. As the heating rate increases, the maximum temperature value of the exothermic peak T_p increases from 1307.99°C to 1329.24 °C.

Figure (III. 9) shows change of $(\frac{\varphi}{T_p^2})$, $ln(\frac{\varphi}{T_p})$ and ln(φ) as function of the inverse of temperature 1/Tp for the formation of cordierite . The values of the activation energy Ea, R and R^2 of the cordierite phase formation are shown in Table (III.1). The values of the activation energy for the formation of cordierite are 1218.12 kJ/mol, 1231.34 kJ/mol and 1183.29 kJ/mol following the Kissinger, Boswell and Ozawa equations, respectively.

Table (III.1) the values of E_a, R and R^2 for cordierite phases.

Method	Ea (KJ/mol)	R	R^2
Ozawa	1183.29	-0.99929	0.99811
Boswell	1231.34	-0.99928	0.99807
Kissinger	1218.12	-0.99926	0.99803

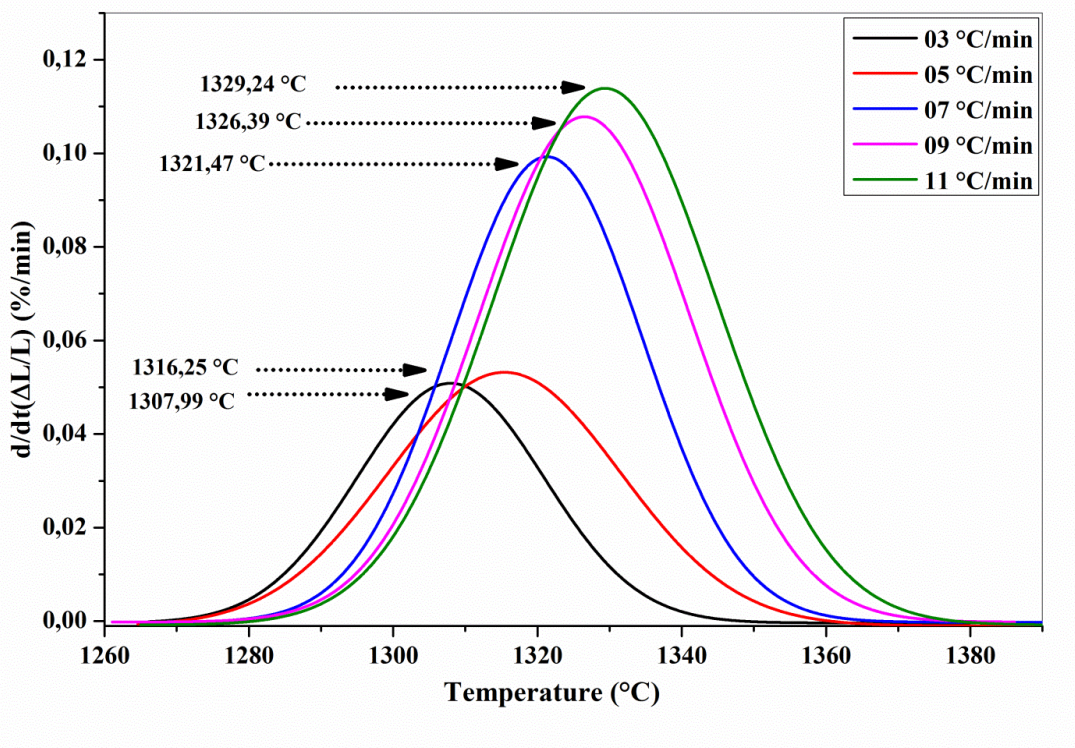

Figure (III. 8) First derivative shrinkage curves for the formation of cordierite at different heating rates.

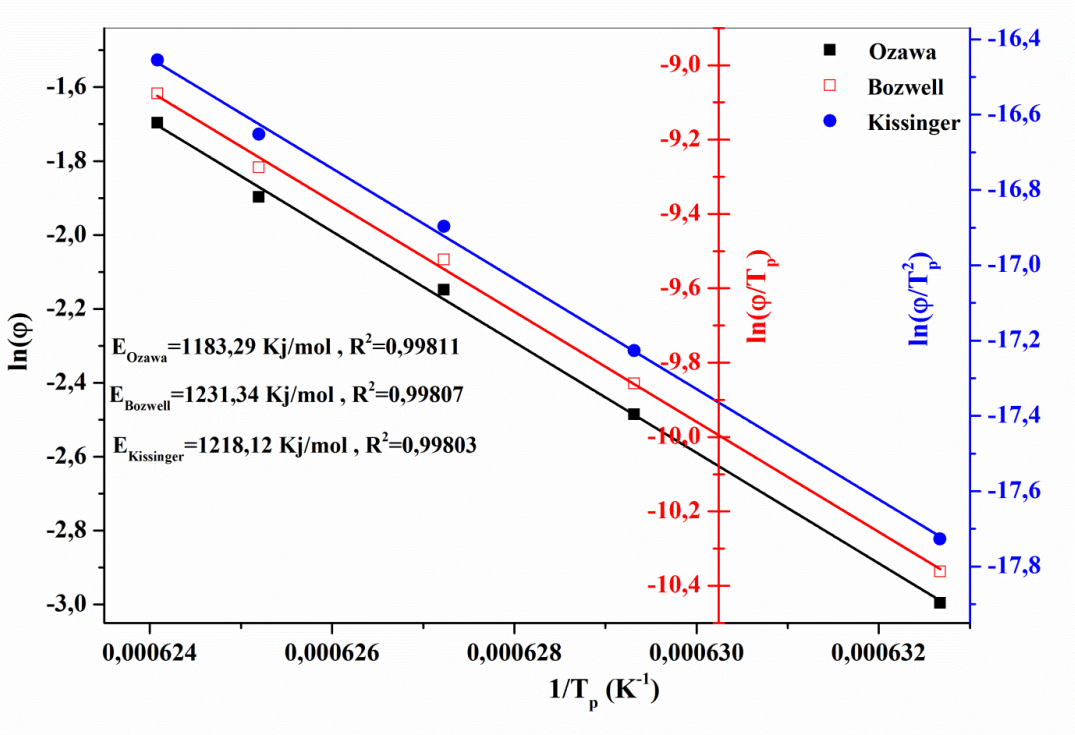

Figure (III. 9) Plots of Y versus (1/Tp) of cordierite formation at various heating rates.

Calculate n

Calculate the value of the exponential parameter Avrami **n** using the following equation (4):

$$n = 2.5\frac{T_p^2}{\Delta T\frac{E_a}{R}} \text{ ..... (4)}$$

The results of calculation are in Table (III.2).

Table (III.2) The parameter value of Avrami n for the cordierite phase.

V	Tp (K)	ΔT(K)	n	n_{moy}
03	1580.99	30.4403	1.40	1.28
05	1589.25	37.6559	1.14	
07	1594.47	31.3345	1.38	
09	1599.39	34.4236	1.27	
11	1602.24	36.4019	1.20	

Calculation of m

The value of the kinetic parameter **m**, which indicates the dimensionality of crystal growth, was calculated using the Matusita equation (Kissinger modified equation)

Matusita equation: $\text{Ln}\left(\frac{\varphi^n}{T_p^2}\right) = -\frac{mE_a}{RT_p} + c$ …… (5)

The figure (III.10) Represent Plot of $\ln\left(\frac{\varphi^n}{T_p^2}\right)$ versus 1/Tp according to Matusita equation, along with Table (III.2), we can note the following:

- ✧ According to Matusita equation, the parameter **m** was found to be **1.32**, and according to equation 4, the parameter $\mathbf{n}_{moy}$ was found to be **1.28,** these values are close to **1.5**.
- ✧ We can conclude that the crystallization mode and the dimensionality of crystal growth of the exothermic peak for cordierite phase during formation is probably three dimensional (polyhedron) diffusion.

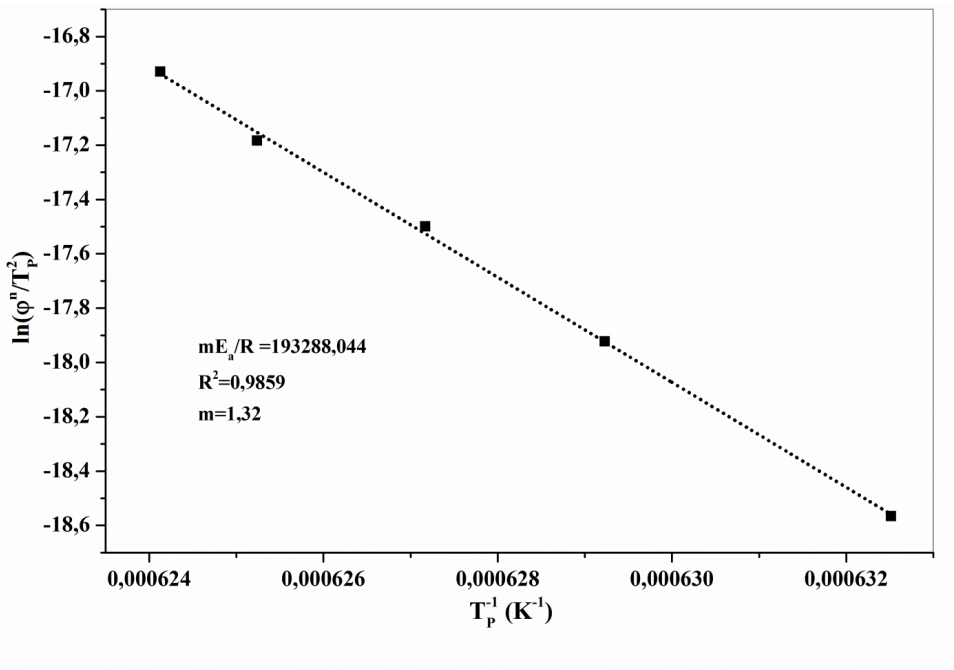

Figure (III.10) Plot of $\ln\left(\frac{\varphi^n}{T_p^2}\right)$ versus 1/Tp according to Matusita equation.

III. 5. 1. 2 Activation energy of Spinel formation using dilatometer

The maximum temperature (Tp), at different heating rates, for the formation of spinel in composite Mullite-cordierite, at different heating rates, Figure (III.11) was obtained from the derivative of the linear shrinkage curve. As the heating rate increases, the maximum temperature value of the endothermic peak T_p value increases from 873.8 °C to 893 °C.

Figure (III. 12) shows change of $(\frac{\varphi}{T_p^2})$, $ln(\frac{\varphi}{T_p})$ and ln(φ) as function of the inverse of temperature 1/Tp for the formation of spinel . The values of the activation energy Ea, R and R^2 of the cordierite phase formation are shown in Table (III.3). The values of the activation energy for the formation of spinel are 722.50 kJ/mol, 732.11 kJ/mol and 705.20 kJ/mol following the Kissinger, Boswell and Ozawa equations, respectively.

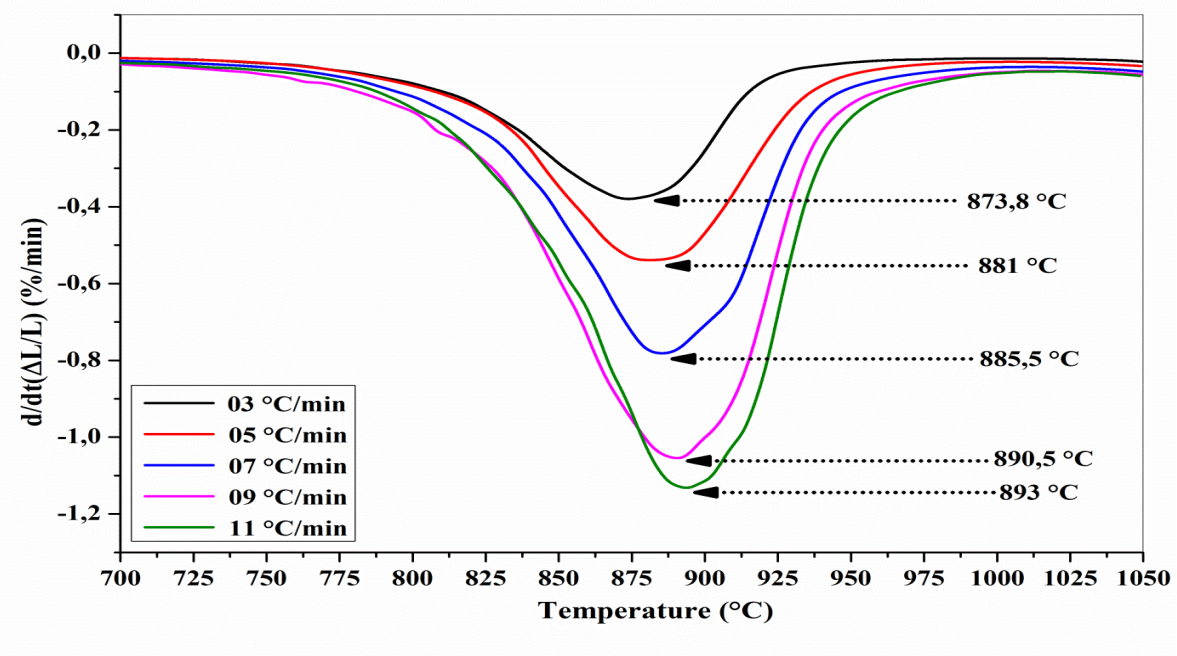

Figure (III.11) First derivative shrinkage curves for the formation of spinel in composite Mullite-cordierite, at different heating rates.

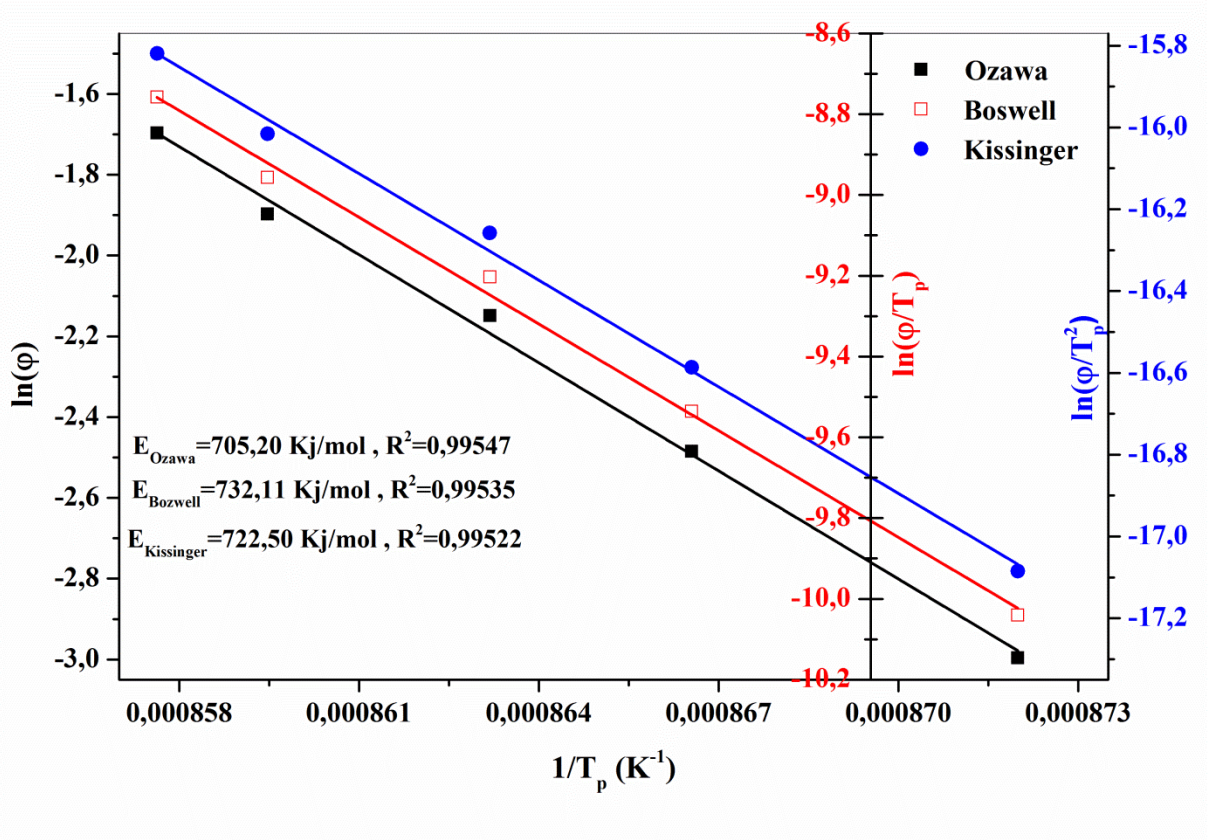

Figure (III.12) Plots of Y versus (1/Tp) of spinel formation at various heating rates.

Table (III.3) the values of E_a, R and R^2 for spinel phases.

Method	**Ea (kJ/mol)**	**R**	**R^2**
Ozawa	705.20	-0.9983	0.99547
Boswell	732.11	-0.99825	0.99535
Kissinger	722.5	-0.99821	0.99522

Calculate n

Calculate the value of the exponential parameter Avrami **n** using the equation (4)

Calculation results are shown in Table (III.4)

Table (III.4) The parameter value of Avrami n for the spinel phase.

V	**Tp (K)**	**ΔT(K)**	**n**	**n_{moy}**
03	1146.8	69.2764	0.55	0.53
05	1154	73.4802	0.52	
07	1158.5	72.0743	0.54	
09	1163.5	76.4994	0.51	
11	1166	74.67619	0.52	

Calculation of m

The value of the kinetic parameter **m**, which indicates the dimensionality of crystal growth, was calculated using the Matusita equation: $\mathrm{Ln}\left(\frac{\varphi^n}{T_p^2}\right) = -\frac{mE_a}{RT_p} + c$ …… (5)

The figure (III.13) Represent Plot of $\mathrm{Ln}\left(\frac{\varphi^n}{T_p^2}\right)$ versus 1/Tp according to Matusita equation, along with Table (III.4), we can note the following:

- ✧ According to Matusita equation, the parameter **m** was found to be **0.517**, and according to equation 4, the parameter $\mathbf{n}_{moy}$ was found to be **0.53,** these values are close to **0.5**.

We can conclude that the crystallization mode and the dimensionality of crystal growth of the endothermic peak for spinel phase during formation is probably One-dimensional (needles) diffusion, and bulk nucleation with constant number of nuclei [40].

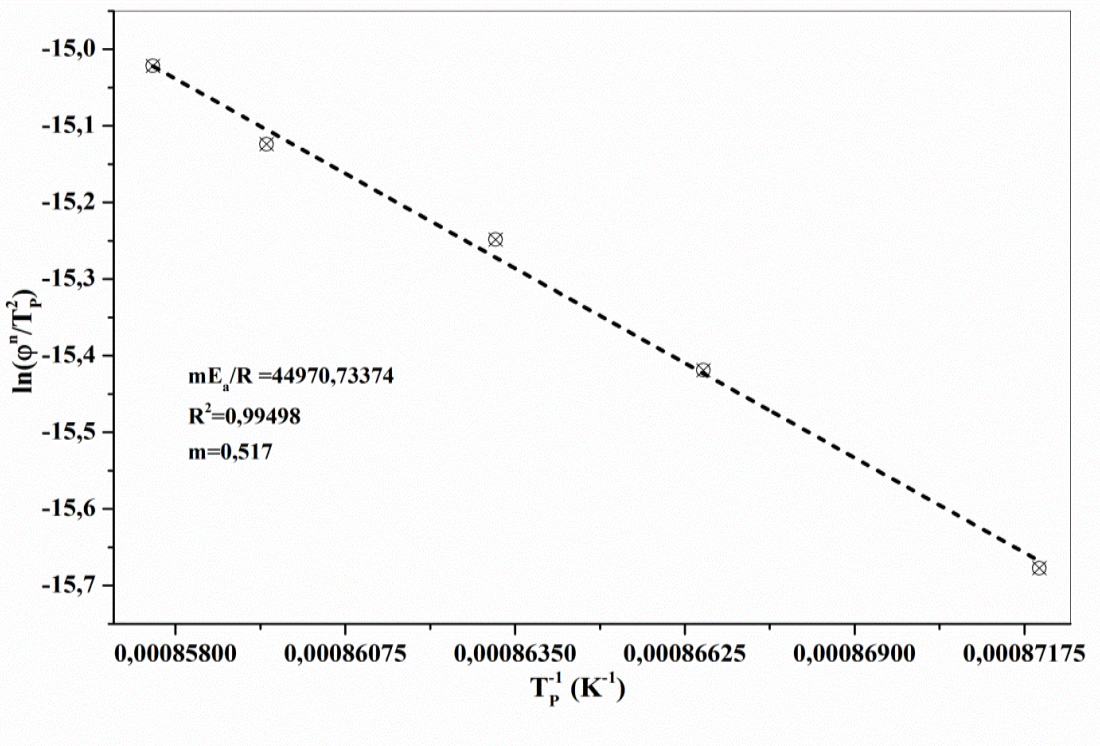

Figure (III.13) Plot of $\ln\left(\frac{\varphi^n}{T_p^2}\right)$ versus 1/Tp according to Matusita equation

III. 5. 2 Isothermal treatment

III. 5. 2. 1 Activation energy of cordierite formation using dilatometer

The variation of crystallised fraction of cordierite with temperature under different heating rates is presented in figure (III.14). The crystallised fraction, x, was determined from dilatometry results as:

$$X = A_T/A_0$$

Where A_T is the area of the peak in the dilatometry curve at temperature T, and A_0 is the total area under the peak. The crystallized fraction, x, at a temperature T differs at different heating rates and hence the curves of dx/dt versus time are also different as shown in figure (III.15), which depicts the growth rate of cordierite with time at different heating rates. The rate of crystallization increases with the increase in heating rate.

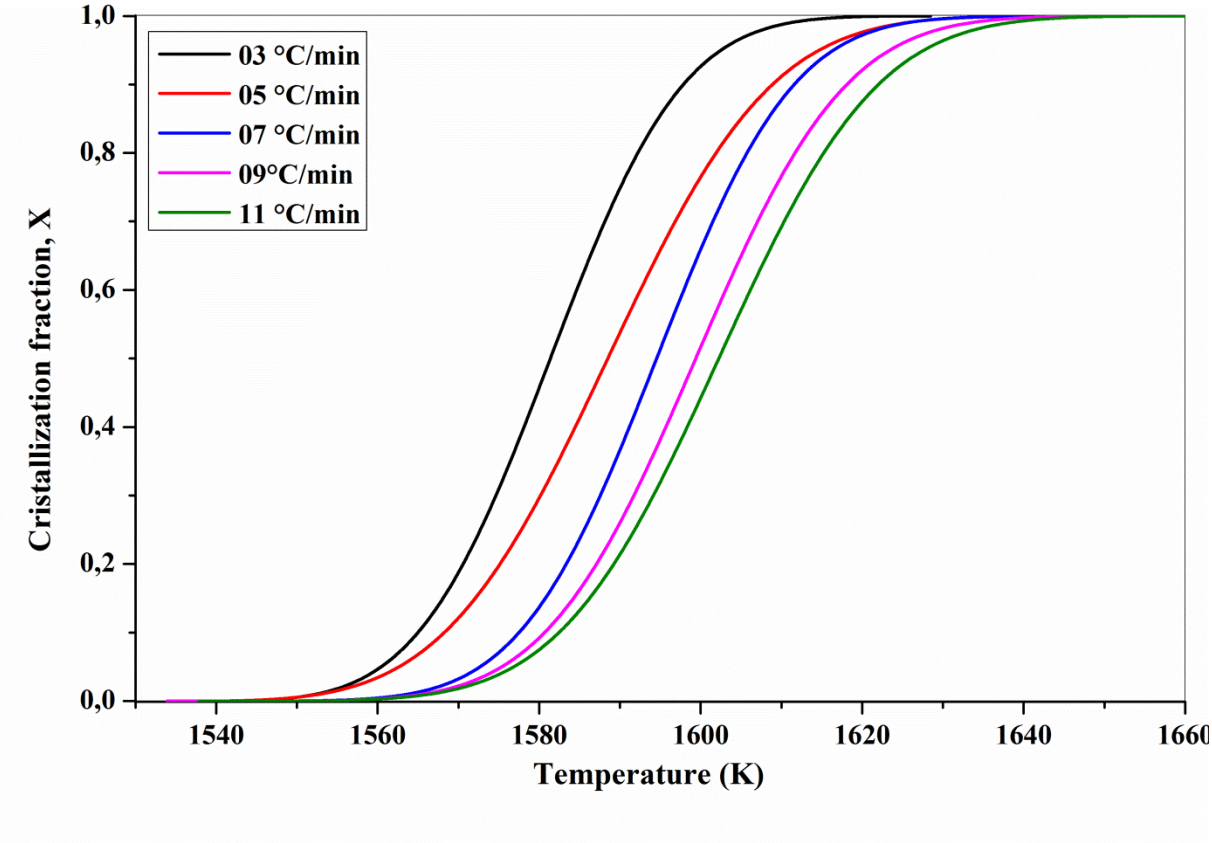

Figure (III.14) Variation of crystallized fraction of spinel, with temperature for M50C50 mixture under different heating rates.

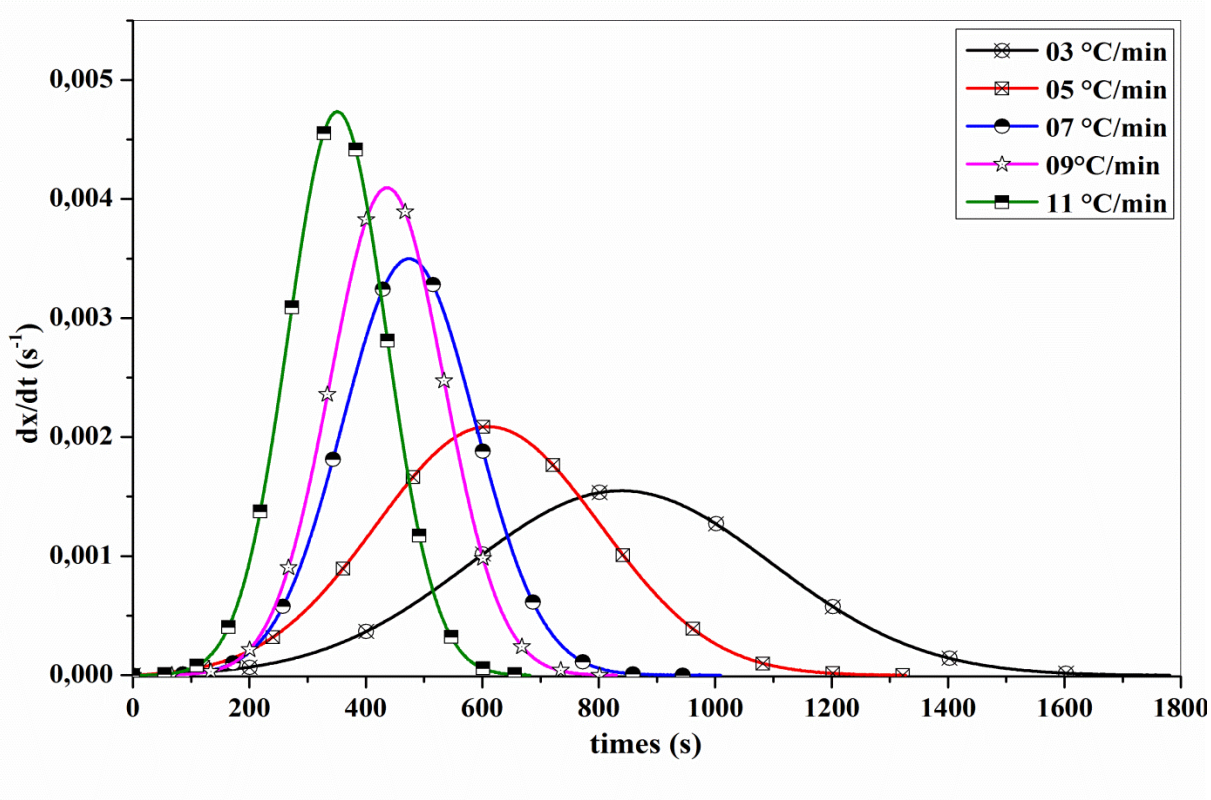

Figure (III.15) The rate of cordierite growth with time, under different heating rates.

Figure (III.16) presents the plot of ln(dx/dt) and 1/T versus crystallized fraction x at different heating rates from dilatometry experiment. A mathematical method through non-isothermal techniques was proposed by LIGERO et al [28]. If the same value of crystallized fraction x in every experiment at different heating rates is selected, the function ln(dx/dt) versus 1/T gives a linear curve (Fig. (III.16)). The values of activation energy, Ea, for different crystallized fractions, which are calculated by the average of the slopes of the lines, are listed in Table (III.5). The coefficient of determination R^2 is greater than 0.99 for different x values. The average activation energy of cordierite phase is 1190.06 kJ/mol, which is in good agreement with that of 1218.12 kJ/mol estimated by non-isothermal DIL treatment.

Table (III.5) Values of the activation energy, Ea, for different values of crystallized fraction.

X	**slop**	**R**	**R*R**	**E**	**E(Kj/mol)**
0.1	-153567.7406	-0.99943	0.99847	1276762.2	1276.76
0.2	-147112.6877	-0.99983	0.99955	1223094.89	1223.09
0.3	-143973.687	-0.99987	0.99966	1196997.23	1197.00
0.4	-140498.9683	-0.99987	0.99966	1168108.42	1168.11
0.5	-137515.9114	-0.99969	0.99918	1143307.29	1143.31
0.6	-136169.6427	-0.99882	0.99685	1132114.41	1132.11
0.7	-134963.3513	-0.99086	0.97574	1122085.3	1122.09
0.8	-130619.7889	-0.98710	0.96582	1085972.93	1085.97
0.9	-124866.9539	-0.98767	0.96732	1038143.86	1038.14

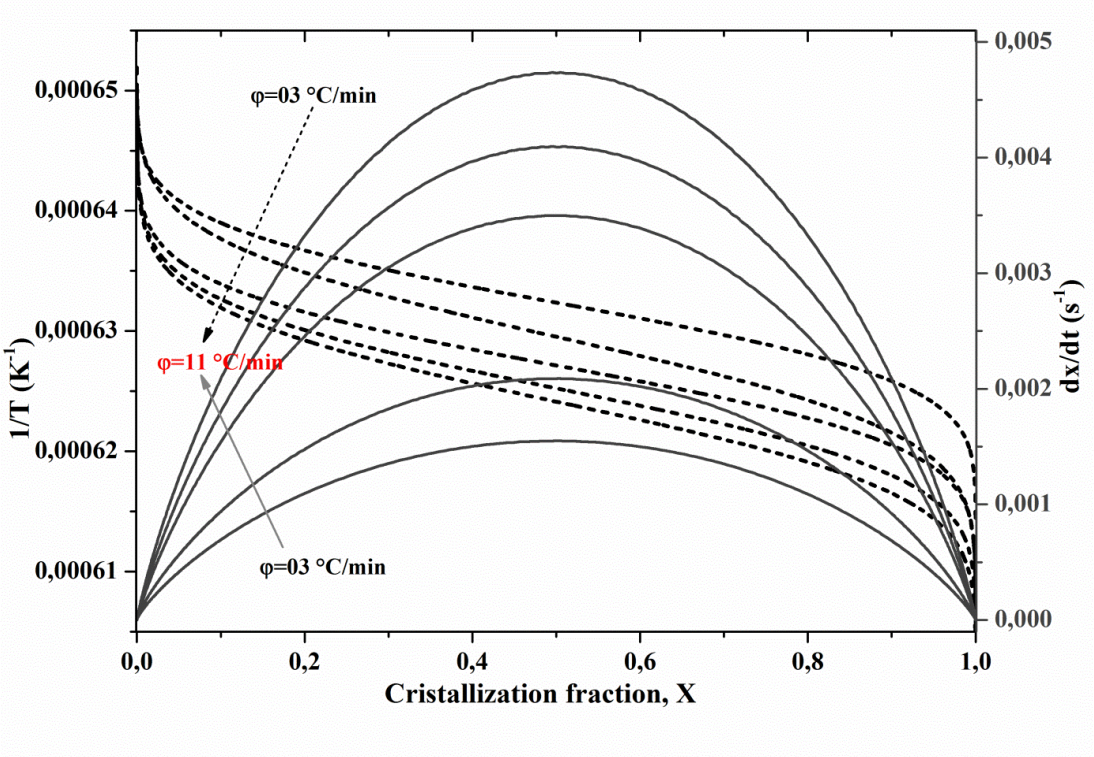

Figure (III.16) Plot of ln(d*x*/d*t*) and 1/*T* versus of crystallized fraction x at different heating rates.

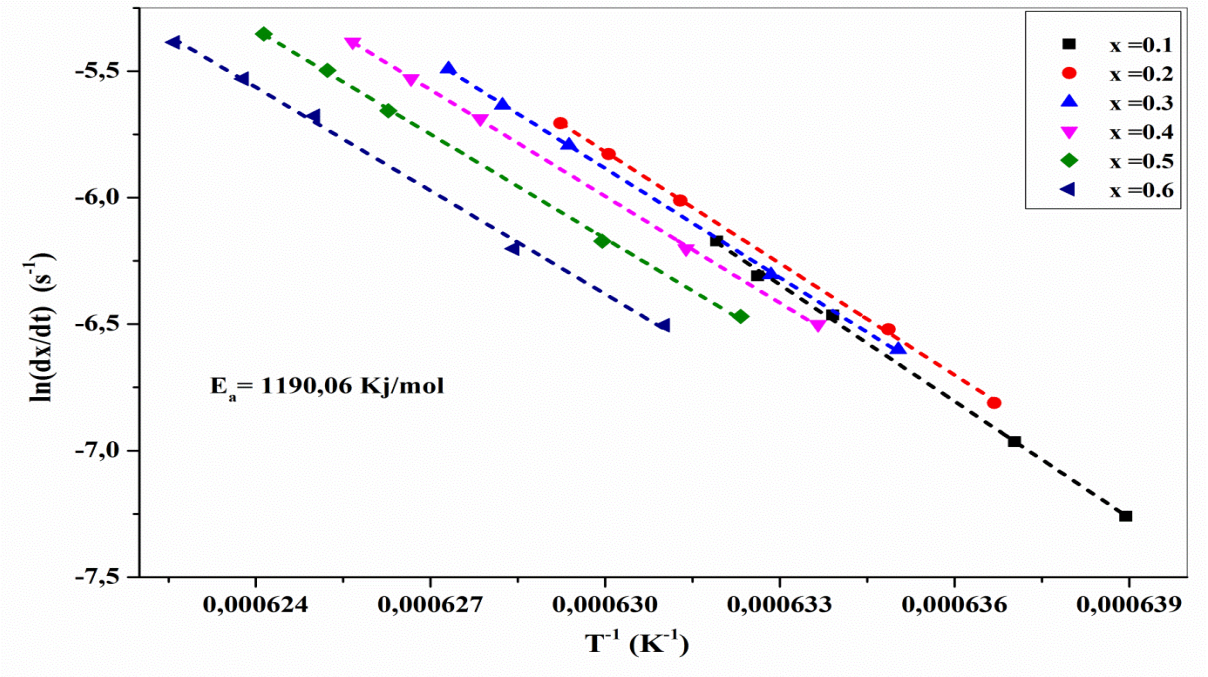

Figure (III.17) Plots of ln(dx/dt) versus 1/T at same value of crystallized fraction x at different heating rates.

Figure (III.18) presents the plot of $\mathrm{Ln}\left(k_0 f(x)\right)$ ln[k_0f(x)] versus crystallization fraction x for a M50C50 mixture heated at a heating rate of 03 °C/min. The Avrami parameter, **n**, was determined by the selection of many pairs of x_1 and x_2 that satisfied the condition $\mathrm{Ln}\left(k_0 f(x_1)\right) = \ln\left(k_0 f(x_2)\right)$. The average values of Avrami parameter, **n**, for each heating rate are listed in Table (III.6). The average Avrami parameter is 1.37. The frequency factor, k_0 calculated by the isothermal treatment is $\mathbf{3.332 * 10^{36}\ (s^{-1})}$.

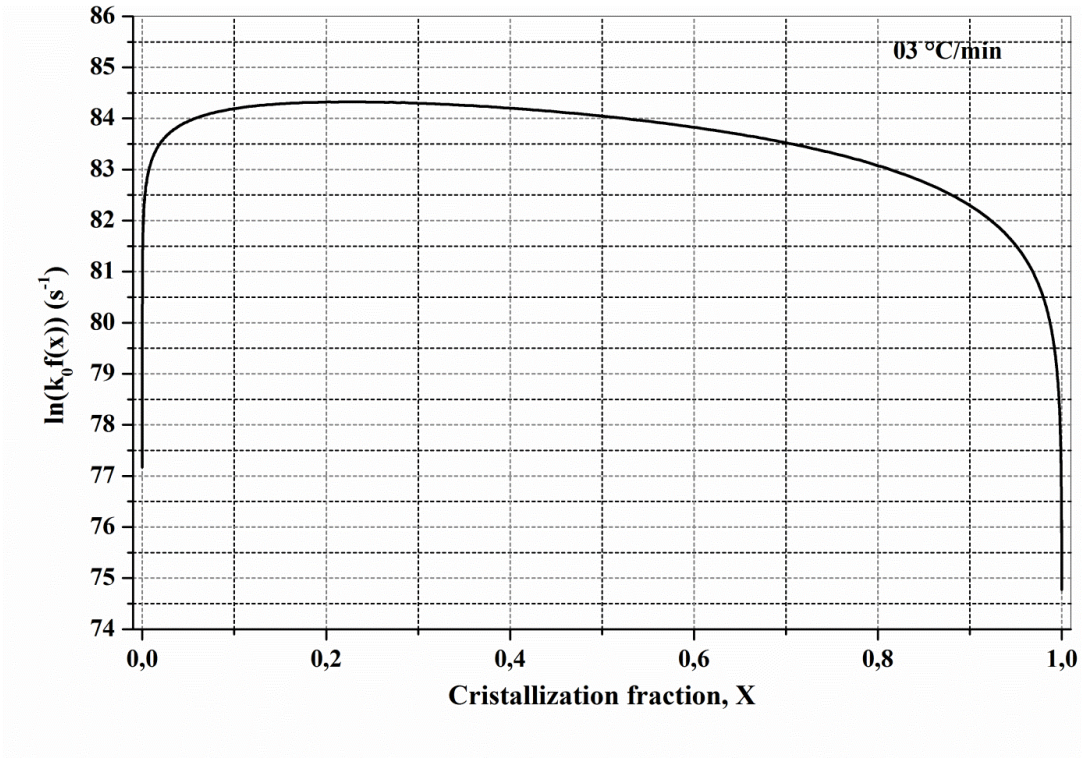

Figure (III.18) Plot of ln(k0f(x)) vs crystallization fraction x for composite mullite-cordierite heated at a heating rate of 03 °C min^{-1}.

Table (III.6) Values of Avrami parameter and frequency factor at different heating rates.

ϑ(°C/min)	n	K0/ 10^{36} (s^{-1})
03	1.40	3.76
05	1.29	3.36
07	1.43	3.45
09	1.41	3.00
11	1.33	3.09
	n_{moy}= 1.37	**$k_{0moy} = 3.332 * 10^{36}$ (s^{-1})**

Figure (III.19) shows the plots of Plot of Ln $\left(\frac{\varphi^n}{T_p^2}\right)$ versus 1/Tp according to Matusita equations. According to Matusita equation, the parameter, **m**, was found to be 1.413 for cordierite formation in M50C50 powder. The parameters, **n,** and, **m**, are both close to 1.5. The bulk nucleation is dominant in cordierite formation followed by three-dimensional growth of cordierite with polyhedron-like morphology controlled by diffusion from a constant number of nuclei.

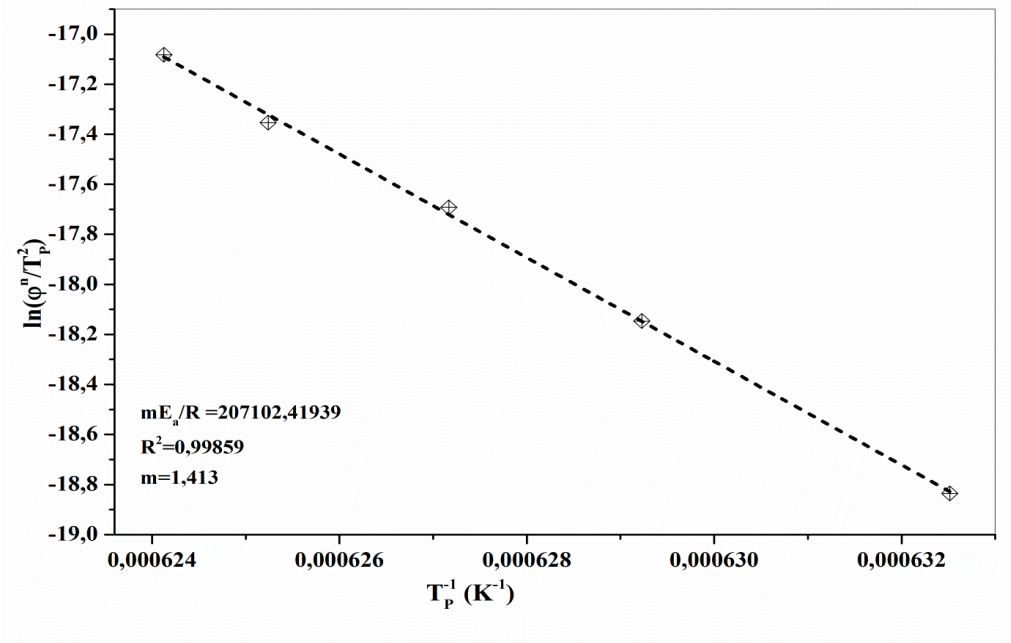

Figure (III.19) Plot of Ln $\left(\frac{\varphi^n}{T_p^2}\right)$ versus 1/Tp according to Matusita equation.

Conclusion

Conclusion

The aim of this work is to study and prepare the cordierite mullite compound by a sol-gel method

In our research we were able to study the phase transformations of the compound cordierite - mullite, and the following results were obtained:

- ✓ Determination of the phases formed at different temperatures and velocities through the results of thermal analysis by the Dilatometric device, through which we found that the formation of phases is related to the treatment temperature and the heating speed by measuring the expansion and contraction of the sample.
- ✓ Determination by X-ray of the phases formed in the powders prepared from the mixture of Cordierite - Mullite, which were treated at different temperatures, it was found that the emergence of the phases formed depends on the temperature of the treatment.
- ✓ Calculation of activation energy using Kissinger, Ozawa and Boswell method to form α-Cordierite stable and spinel and calculate the kinetic factors controlling the growth and nucleation mechanism (Avrami factor n and numerical parameter m).

In the end, we can say that we were able to determine the phases forming the compound corderite - mullite, and we were able to determine the factors controlling the obtaining of the compound corderite - mullite by using laboratory devices.

Reference

1. M. W. Barsoum, Fundamentals of Ceramics, © IOP Publishing Ltd 2003.
2. M. VALÁŠKOVÁ , "CLAYS, CLAY MINERALS AND CORDIERITE CERAMICS - A REVIEW", Ceramics – Silikáty 59 (4) 331-340 (2015).
3. F. A. Costa Oliveira, L. G. Rosa, J. C. Fernandes, J. Rodrı´guez, I.Can˜adas, D. Martı´nez and N. Shohoji1, Mechanical Properties of Dense Cordierite Discs Sintered by Solar Radiation Heating, Materials Transactions, Vol. 50, No. 9 (2009) 2221-2228.
4. M. D. Karkhanavala and F. A. Hummel, "The Polymorphism of Cordierite", journal of the American Ceramic Society, VOL. 36, NO. 12 (1953) 389-392.
5. Philippe Boch, Jean Claude Niépce, "Ceramic Materials : Processes, Properties and Applications", United States, P.214-205,(2007).
6. S. Sembiring, W. Simanjuntak, R. Situmeang, Agus Riyanto and Junaidi, "structural and physical properties of refractory cordierite precursors prepared from rice husk silica with different MgO addition" Ceramics-Silikáty 62 (2), 163-172 (2018)
7. Soumya Sourav Patra, Synthesis and Characterization of Cordierite-Based Vitreous Ceramics, Master degree, ROURKELA: national institute of technology, p. 11.
8. S. Mei, J. Yang and J.M.F Ferreira, "Cordierite-based glass-ceramics processed by slip casting" Journal of the European Ceramic Society 21 (2001) 185-193.
9. A. Chowdhury, S. Maitra, H.S. Das, A. Sen, G.K. Samanta and P. Datta, Synthesis, Properties and Applications of Cordierite Ceramics, Part 2". InterCeram 8 Vol. 56 (2007) [2]
10. K. Kobayashi, K. Sumi and E. Kato, "Preparation of dense cordierite ceramics from magnesium compounds and kaolinite without additives", Ceramics International, Ceramics International 26 (2000) 739-743
11. M. A. Cameruccia, G. Urretavizcaya and A. L. Cavalieri, "Sintering of cordierite based materials", Ceramics International 29 (2003) 159–168.
12. R. Goren, C. Ozgur and H. Gocmez, "Synthesis of cordierite powder from talc, diatomite and aluminain, ceramics International, Ceramics International 32 (2006) 53-
13. J. Zhou, Y. Dong, S. Hampshire and G. Meng "Utilization of sepiolite in the synthesis of porous cordierite ceramics, Applied Clay Science, 52 (2011) 328-332.

14. E. P. Almeida, I. P. Brito, H. C. Ferreira, H. L. de Lucena, L. N. de Lima Santana and G. de Araujo Neves "Cordierite obtained from compositions containing kaolin waste, talc and magnesium oxide", Ceramics International 44 (2) (2018). 1719-1725.
15. R. Li, A. E. Clark, L. L. Hench, "An Investigation of Bioactive Glass Powders by Sol-Gel Processing", Journal of Applied Biomaterials, Vol 2 (1991) 231 239.
16. James F. Shackelford and Robert H. Doremus, "Ceramic and Glass MaterialsStructure, Properties and Processing" © 2008 Springer Science+Business Media, LLC.
17. S. Aramakl and R. Roy, "Revised Phase Diagram for the System A12O3-SiO2", Journal of the American Ceramic Society, Vol. 45, No. 5 (1962) 229-242.
18. I. A. Aksay, D. M. Dabbs, M.t Sarikaya*, Mullite Processing, Structure, and Properties :Mullite for Structural, Electronic, and Optical Applications, J. Am. Cerom. Soc., 74 [10] (1991) 2343-58 .
19. H. Schneider, R. X. Fischer and J. Schreuer, "Mullite: Crystal Structure and Related Properties", J. Am. Ceram. Soc., 98 [10] 2948–2967 (2015).
20. Juliana Anggono, "Mullite Ceramics: Its Properties, Structure, and Synthesis", Jurnal Teknik Mesin Vol. 7, No. 1, April (2005) 1-10.
21. H. Schneider, J. Schreuer and B. Hildmann, "structure and properties of mullite-A review", Journal of the European Ceramic Society 28 (2008) 329–344.
22. K. K. Chawla, Z. R. Xu and J.-S. Ha, "Processing, Structure, and Properties of Mullite Fiber/Mullite Matrix Composites ",Journal of the Europenn Ceramic Society 16 (1996) 293-299.
23. A. A. Albhilil, M. Palou and J. Kozánková, "Characterization of cordierite-mullite ceramics prepared from natural raw materials", Acta Chimica Slovaca, Vol. 6, No. 1 (2013) 1-7.
24. Ankita Bilung, "Synthesis and Characterization of Cordierite-Mullite Composite", Nation Institute of technology, Diploma 2012, P.10.
25. P. Kiattisaksophon and S. Thiansem, "The Preparation of Cordierite-Mullite Composite for Thermal Shock Resistance Material, Chiang Mai J.Sci. 35 No.1 (2008) 6-10.
26. Mohamed G. M. U. Ismail, H. Tsunatori, and Z. Nakai, "Preparation of Mullite Cordierite Composite Powders by the Sol-Gel Method: Its Characteristics and Sintering ", J. Am. Ceram. Soc ,73, 31(1990) 537-43.
27. M. Romeo, J. Martín-Márquez, J. Ma. Rincón, "Kinetic of mullite formation from a

porcelain stoneware body for tiles production", J. Euro. Ceram. Soc., 26 (2006) 1647-1652.

28. R. A. LIGERO, J. VAZQUEZ, P. VILLARES, R. JIMENEZ-GARAY, study of the crystallization kinetics of some Cu−As−Te glasses. Journal of Materials Science, 26 (1991) 211−215.
29. T. Ozawa, "A new method of analyzing thermogravimetric data",. Bulletin of the chemical society of Japan , 38 (11) (1965) 1881-1886.
30. P. G. Boswell, "On the calculation of activation energies using a modified Kissinger method",. Journal of Thermal Analysis, VoL 18 (1980) 353- 358.
31. R. Petrovic´, Dj. Janackovic, S. Zec, S. Drmanic´ and Lj. Kostic´-Gvozdenovic, "Phase-transformation kinetics in triphasic cordierite gel, J. Mater. Res., Vol. 16, No. 2 Feb (2001) 451-458.
32. Hongbing tan, yapping ding , jianfeng yan, mullite fibres preparation by aqueous sol gel process and activation energy of mullitization ,(2009).
33. Ki Chang Song, "Preparation of mullite fibers from aluminum isopropoxide–aluminum nitrate–tetraethylorthosilicate solutions by sol–gel method, Materials Letters 35 1998 290–296.
34. D. Voll and A. Beran, "Dehydration process and structural development of cordierite ceramic precursors derived from FTIR spectroscopic investigations", Phys Chem Minerals 29 (2002) 545–551.
35. I. Jankovic´-C˘astvan*, S. Lazarevic, D. Tanaskovic, A. Orlovic´, R. Petrovic´ and Dj. Janac´kovic, "Phase transformation in cordierite gel synthesized by non-hydrolytic sol–gel route", Ceramics International 33 (2007) 1263–1268.
36. M. S. Kumar, A. E. Perumal, T. R. Vijayaram and G. Senguttuvan, "Processing and characterization of pure cordierite and zirconia-doped cordierite ceramic composite by precipitation technique",. Bull. Mater. Sci., Vol. 38, No. 3, June (2015) 679–688.
37. V. S. NAGARAJAN and K. J. RAO, "reparation and Thermal Evolution of the Microstructure of Sol-Gel-Derived Cordierite and Cordierite-Zirconia Powders" , JOURNAL OF SOLID STATE CHEMISTRY 94, 149-162 (1991).
38. P. Padmaja, G.M. Anilkumar, P. Mukundan, G. Aruldhas, K.G.K. Warrier, "Characterisation of stoichiometric sol–gel mullite by fourier transform infrared spectroscopy", International Journal of Inorganic Materials 3 (2001) 693–698.
39. S. Wattanasiriwecha, , F. Arif Nurgesang , D. Wattanasiriwech and P. Timakul, "Characterisation and properties of geopolymer composites. Part 2: Role of

cordierite-mullite reinforcement, Ceramics International,Volume 43, Issue 18, 15 December (2017)16055-16062.

40. D. PAL, A. K. Chakraborty, S. Sen and S. K. Sen, "The synthesis, characterization and sintering of sol-gel derived cordierite ceramics for electronic applications", Journal of Materials Science 31 (1996) 3995-4005.
41. A. Sundar Majumdar and G. Mathew, "Raman-Infrared (IR) Spectroscopy Study of Natural Cordierites from Kalahandi, Odisha", journal geological society of india , Vol.86, July (2015).80-92 .
42. J. Roy, N. Bandyopadhyay, S. Das and S. Maitra, "Studies on the Formation of Mullite from Diphasic Al2O3-SiO2 Gel by Fourier Transform Infrared Spectroscopy", Iran. J. Chem. Chem. Eng, Vol. 30 No. 1 (2011) 65-71.
43. Nikita V. Chukanov and Alexandr D. Chervonnyi, "Infrared Spectroscopy of Minerals and Related Compounds", © Springer International Publishing Switzerland 2016.

الملخص

تم تحضير مركب الميليت – كورديريت بطريقة المحاليل الغروية، و ذلك باستخدام مسحوق نترات المغنيسيوم و نترات الالومنيوم ومحلول تيترايثيل أورثوسيليكات كمواد أولية ، أين تم خلط هذه المواد بنسب مختلفة حسب الصيغة الستكيومترية للمركب المراد الحصول عليه، و لتحليل المواد المحضرة استخدمنا عدة تقنيات في التحليل منها التحليل الحراري الكتلي والتحليل الحراري التفاضلي TG/DSC، وكذا التحليل بواسطة مقياس التمدد الحراري (Dilatometry) وهذا لأجل مراقبة التحولات الطورية، و لتأكيد ذلك استخدمنا تقنية التحليل بواسطة حيود الاشعة السينية (XRD) و التي بها تم معرفة الأطوار المتشكلة في المركب M50C50 و هي الميليت و الكورديريت، كما تتبعنا مراحل التحول الطوري للمساحيق M50C50 المعالجة بواسطة مقياس التمدد الحراري (Dilatometry) عند مختلف درجات الحرارة بتقنية التحليل بواسطة إنعراج الأشعة السينية ، أين استطعنا بواسطة بطاقات العناصر ان نتعرف على الأطوار المتشكلة بمختلف درجات الحرارة ، كما تم حساب طاقة التنشيط ومعاملات أفرامي للنمو و التنوي لطور الكورديريت في حالة تغير درجة الحرارة و ثبوتها و للسبينال Al-Si في حالة تغير درجة الحرارة باستخدام نتائج التحليل لمقياس التمدد الحراري، اين تحصلنا على قيم الطاقة التالية: 1210.91 kJ/mol و 1190.06 kJ/molعلى الترتيب بالنسبة للكورديريت، و 719.93 kJ/mol بالنسبة للسبينال، أما قيمة معاملات النمو المرفولوجي n و m فهي تقارب 1.5 مما يشير إلى أن حجم التنوي السائد في تشكل طور الكورديريت متبوعا بنمو ثلاثي الأبعاد لبلورات الكورديريت مع شكل يشبه متعدد السطوح يتم التحكم فيه عن طريق الانتشار من عدد ثابت من النوى. أما بالنسبة للسبينال فهي تقارب 0.5 مما يشير إلى أن حجم التنوي السائد في تشكل طور سبينال متبوعا بنمو في بعدين مع شكل صفائحي يتم التحكم فيه عن طريق الانتشار من عدد ثابت من النوى.

كلمات مفتاحية: ميليت- كورديريت، محاليل هلامية، طاقة التنشيط، معاملات أفرامي.

Abstract

The mullite-cordeirite composites was prepared by Sol-Gel method, using magnesium nitrate powder, aluminum nitrate powder and tetraethyl orthosilicate solution as raw materials, these materials were mixed in various ratios according to stoichiometric formula of the wanted composite, in order to analyze the prepared materials we used several techniques, including Thermogravimetry and Differential Thermal Analysis (TG/DSC), also Dilatometry analysis to observe the phases transformation, and to confirm it we used X-ray diffraction analysis (DRX) which it been used to identify the formed phases of M50C50 which is mullite and cordierite, we also tracked the stages of phase transformations for M50C50 powder that has been treated by Dilatometry at various temperatures using the analysis technique by X-ray diffraction, where we were able by means of the ASTM cards , to identify the formed phase in various temperatures, and activation energy and Avrami parameters for cordierite phase in the non-isothermal and isothermal treatment, and for Al-Si spinal phase in the non-isothermal, were calculated based on Dilatometry analysis results, we found that the energy as the following: 1210.91 kJ/mol and 1190.06 kJ/mol respectively for cordierite and 719.93 kJ/mol for spinel, as for the morphological growth parameters n and m are approximately 1.5 which indicating that the dominant crystallization volume mode in cordierite phase formation followed by three dimensional growth of spinal crystals with a polyhedral-like shape controlled by diffusion from fixed number of nuclei, As for the spinal, it is approximately 0.5, indicating that the dominant crystallization volume mode in a spinal phase formation followed by one-dimensional (needles) diffusion, and bulk nucleation with constant number of nuclei.

Keywords : Mullite, Cordierite, Sol-Gel, Activation Energy, Avrami parameters.